

# Metallomics

Accepted Manuscript



This is an *Accepted Manuscript*, which has been through the Royal Society of Chemistry peer review process and has been accepted for publication.

*Accepted Manuscripts* are published online shortly after acceptance, before technical editing, formatting and proof reading. Using this free service, authors can make their results available to the community, in citable form, before we publish the edited article. We will replace this *Accepted Manuscript* with the edited and formatted *Advance Article* as soon as it is available.

You can find more information about *Accepted Manuscripts* in the [Information for Authors](#).

Please note that technical editing may introduce minor changes to the text and/or graphics, which may alter content. The journal's standard [Terms & Conditions](#) and the [Ethical guidelines](#) still apply. In no event shall the Royal Society of Chemistry be held responsible for any errors or omissions in this *Accepted Manuscript* or any consequences arising from the use of any information it contains.

Cite this: DOI: 10.1039/c0xx00000x

www.rsc.org/xxxxxx

ARTICLE TYPE

## Selective anticancer copper(II)-mixed ligand complexes: targeting of both ROS and proteasome

Chew Hee Ng,<sup>\*a</sup> Siew Ming Kong,<sup>b</sup> Yee Lian Tiong,<sup>c</sup> Mohd Jamil Maah,<sup>d</sup> Nurhazwani Sukram,<sup>e</sup> Munirah Ahmad,<sup>e</sup> and Alan Soo Beng Khoo<sup>e</sup>

Received (in XXX, XXX) Xth XXXXXXXXX 20XX, Accepted Xth XXXXXXXXX 20XX

DOI: 10.1039/b000000x

Copper compounds can be alternatives to platinum-based anticancer drugs. This study investigated the effects of a series of ternary copper(II) complexes, [Cu(phen)(aa)(H<sub>2</sub>O)]NO<sub>3</sub>.xH<sub>2</sub>O **1-4** (phen = 1,10-phenanthroline; aa = gly (**1**), DL-ala (**2**), sar (**3**), C-dmg (**4**)), on metastatic and cisplatin-resistant MDA-MB-231 breast cancer cells and MCF10A non-cancerous breast cells, and some aspects of the mechanisms. These complexes were distinctively more antiproliferative towards and induced greater apoptotic cell death in MDA-MB-231 than in MCF10A cells. **2** and **4** could induce cell cycle arrest only in cancer cells. Further evidence from DCFH-DA assay showed higher induction of reactive oxygen species (ROS) in treated cancer cells but minimal ROS increase in normal cells. DNA double-strand breaks, *via* a  $\gamma$ -H2AX assay, were only detected in cancer cells treated with 5  $\mu$ M of the complexes. These complexes poorly inhibited chymotrypsin-like activity in 20S rabbit proteasome while they did not inhibit the three proteolytic sites of MDA-MB-231 cells at 10  $\mu$ M. However, the complexes could inhibit degradation of ubiquitinated proteins of MDA-MB-231 cells. In addition, compound **4** was found to be effective against cervical (Hela), ovarian (SKOV3), lung (A549, PC9), NPC (Hone1, HK1, C666-1), breast (MCF7, T47D), lymphoma leukemia (Nalmawa, HL60) and colorectal (SW480, SW48, HCT118) cancer cell lines with IC<sub>50</sub> values (24 h) in the 1.7 – 19.0  $\mu$ M range. Single dose NCI60 screening of **4** showed the complex to be highly cytotoxic to most cancer cell types and more effective than cisplatin.

### Introduction

Increasing efficacy and reducing the harmful side effects of a potential drug are central issues in anticancer drug development. Collateral killing of normal cells by anticancer drugs is an important cause of side effects. Although relatively successful, cisplatin is not widely used because of cell resistance and its toxic side effects.<sup>1,2</sup> Thus, new metal-based anticancer agents with selectivity against cancer cells are needed. Due to elevated copper levels and higher oxidative stress in cancer cells, compounds which target the redox process and thereby modulate intracellular ROS levels could be useful.<sup>3,4</sup> A ROS-inducing compound,  $\beta$ -phenylethyl isothiocyanate (PEITC), was found to selectively kill the transformed cells but not normal cells, suggesting the possibility of using this strategy for improving the selectivity against cancer cells.<sup>5</sup> This was explained by reaching of the “ROS threshold of initiation of apoptosis” only in cancer cells. However, the possibility of such selective ROS-induced apoptosis by copper(II) complexes has not been extensively explored. An inorganic compound, (4,7-dimethyl-1,10-phenanthroline)(glycinato)-copper(II), was found to inhibit 70% growth of normal monkey kidney cells at 50  $\mu$ M *via* cell death caused mainly by ROS induced by the copper(II) complex.<sup>6</sup>

However, the corresponding data and proposed mechanism of this complex on the murine leukemia cell line L1210 was not provided. Although Filomeni *et al* reported that two isatin-Schiff base copper(II) complexes could induce cell cycle arrest and apoptosis in human neuroblastoma cells SH-SY5Y mainly by copper-dependent oxidative stress and nuclear/mitochondrial site-directed damage, no normal cells were tested.<sup>7</sup> Subsequently, it was found that a copper complex of N-(2-hydroxyacetophenone)glycinate killed doxorubicin-resistant leukemia cells *via* ROS-induced apoptosis but did not harm normal cells.<sup>8</sup>

Inhibition of proteasome is another potentially useful strategy for anticancer therapy. The proteasome is an abundant multicatalytic protein complex in eukaryotic cells that degrades intracellular proteins which are not needed anymore, misfolded or damaged. It controls the levels of proteins that are important for many important cellular processes, including cell growth, cell-cycle progression and apoptosis in normal and malignant cells.<sup>9,10</sup> Although the various proteasome-inhibition mechanisms are not well understood, it seems feasible to target the proteasome as empirical evidence showed that various types of cancer cells were more sensitive to proteasome inhibition than noncancerous cells.<sup>9</sup>

1 Many natural and synthetic classes of organic compounds could  
2 inhibit proteasome. In spite of this, only bortezomid and the  
3 better second generation carfilzomid have been approved for  
4 clinical treatment and mainly for relapsed/refractory multiple  
5 myeloma.<sup>11</sup> Unfortunately, both treatments have numerous  
6 adverse side effects, such as resistance, haematological and  
7 neurological complications.<sup>11,12</sup> The toxicities in patients treated  
8 with bortezomid can be attributed to a lack of selectivity in its  
9 activity in cancer cells over normal cells.<sup>13</sup> There has been few  
10 reports of proteasome inhibition by copper(II) complexes.  
11 However, copper-containing compounds are only in the early  
12 preclinical stage of development as anticancer agents. Dou *et al*  
13 found that *bis*(8-hydroxyquinoline)copper(II), [Cu(8OHQ)<sub>2</sub>], and  
14 other copper(II) compounds were able to inhibit the proteasome  
15 and induce apoptosis.<sup>14</sup> Subsequently, other copper(II)  
16 compounds were reported to have similar activities.<sup>10,15-16</sup> The  
17 choice of the ligand or the substituent on the ligand appeared  
18 crucial for the proteasome inhibiting activity. For example,  
19 copper(II) complexes with either a 7-iodo-8-hydroxy-quinoline-  
20 5-sulfate (8-OHQ-1-S-Cu) or a strong chelator like  
21 ethylenediaminetetraacetic acid (EDTA) were not able to inhibit  
22 the proteasome. Nevertheless, some copper(II) complexes were  
23 later found to be able to selectively inhibit 20S proteasome  
24 activity in cancer cells but not in normal cells, and induce more  
25 pronounced apoptosis in cancer cells over normal cells based on  
26 morphological observations.<sup>17</sup> Numerous anticancer copper(II)  
27 complexes were not tested for proteasome inhibition.<sup>10</sup> The  
28 above review prompted us to investigate whether our previously  
29 synthesized [Cu(phen)(aa)(H<sub>2</sub>O)]NO<sub>3</sub>·xH<sub>2</sub>O (phen = 1,10-  
30 phenanthroline; aa = methylated glycine (sarcosine, sar; DL-  
31 alanine, DL-ala; 2,2-dimethylglycine, C-dmg)<sup>18,19</sup> could induce  
32 apoptosis *via* both ROS generation and proteasome inhibition.

33 Among the various types of cancer, breast cancer is the most  
34 prevalent and is the leading cause of cancer death among  
35 women.<sup>20</sup> Despite recent increase in understanding of its biology  
36 and development of new therapies, metastatic breast cancer is  
37 incurable and the number of years of survival of patients with  
38 metastatic cancer remain low.<sup>21,22</sup> Consequently, we used  
39 metastatic breast cancer cells MDA-MB-231 and the  
40 corresponding non-malignant ("normal") cells MCF10A to test  
41 our copper(II) complexes for selectivity against breast cancer.

## 42 Experimental

### 43 Chemicals and cell culture

44 The synthesis of [Cu(phen)(aa)(H<sub>2</sub>O)]NO<sub>3</sub> complexes (aa = gly,  
45 DL-ala, sar, C-dmg) was similar to a previously published  
46 method.<sup>19</sup> Briefly, Cu(NO<sub>3</sub>)<sub>2</sub> was reacted with phen, and an  
47 appropriate amino acid in the presence of aqueous NaOH. All  
48 reagents used were of analytical grade and used as such.  
49 Copper(II) 8-hydroxyquinoline complex [Cu(8OHQ)<sub>2</sub>] was  
50 obtained from Sigma-Aldrich (St. Louis, MO) and was used  
51 directly. Cell culture products were purchased from Invitrogen  
52 (Grand Island, NY). FITC Annexin V Apoptosis Detection Kit II,  
53 Alexa Fluor® 488 Mouse anti-H2AX (pS139), PI and Alexa  
54 Fluor® 488 Mouse IgG1 κ Isotype Control were purchased from  
55 BD Biosciences (MA, USA). Ubiquitin (P4D1) and IκB-α (C-15)

antibodies were purchased from Santa Cruz Biotechnology (Santa  
Cruz, CA). β-actin antibody was purchased from Cell Signaling  
(MA, USA). Insulin, hydrocortisone, DMSO (dimethyl  
sulfoxide), DCFH-DA, BSA (bovine serum albumin) and MTT  
were purchased from Sigma-Aldrich (St. Louis, MO).  
SuperSignal West Pico Chemiluminescent Substrate was  
purchased from Thermo Scientific (Rockford, USA). Western  
Lighting™ Chemiluminescence Reagent Plus was purchased  
65 from PerkinElmer (MA, USA). A substrate for the chymotrypsin-  
like activity of the proteasome, Suc-Leu-Leu-Val-Tyr-AMC  
(AMC, 7-Amino-4-methylcoumarin) and 20S rabbit proteasome  
were purchased from Calbiochem. Proteasome-Glo™  
Chymotrypsin-like, Trypsin-like and Caspase-like cell based  
70 assay was obtained from Promega. Dulbecco's modified eagle  
medium (DMEM) and F12 growth medium were from GIBCO®.  
Breast cancer (MDA-MB-231) and immortalized human  
mammary epithelial (MCF10A) cell lines (American Type  
Culture Collection (ATCC), (Manassas, VA, USA)). MCF 10A  
75 cells were cultured in 1:1 DMEM/F12 growth medium while  
MDA-MB-231 cells were cultured in DMEM medium  
supplemented with 10 % heat-inactivated fetal calf serum (FCS),  
50 U/mL penicillin and 50 µg/mL streptomycin in a humidified  
atmosphere containing 5% CO<sub>2</sub>. Cell counts and viability counts  
80 were determined by Countess® Automated Cell Counter  
(Invitrogen).

### MTT assay

85 Cell viability of MDA-MB-231 and MCF10A cells was  
determined using the MTT assay as previously described.<sup>19</sup> Cells  
were seeded at density 1 × 10<sup>5</sup> cells/mL in 100 µL medium per  
well and incubated at 37 °C in a 5 % CO<sub>2</sub> incubator overnight  
before been treated with each test compound (copper(II)  
90 complexes (1-4) and [Cu(8OHQ)<sub>2</sub>]) at six different test drug  
concentrations (25.00 µM, 12.50 µM, 6.25 µM, 3.12 µM and  
1.56 µM). After further incubation for 24 h under the same  
conditions, the cells were treated with 5 mg ml<sup>-1</sup> MTT solution  
and incubated for another 4 h. The cell monolayer in each cell  
95 was added with 100 µL DMSO to dissolve the formazan formed  
and the optical density of each well was measured with an ELISA  
plate reader (Dynatech MRX) at a wavelength of 570 nm with  
background subtraction at 630 nm. Cell viability of treated  
samples was calculated in reference to the untreated control that  
100 was defined as 100% viability. IC<sub>50</sub> values (the concentration of  
the complex causing 50 % growth inhibition) were estimated  
from dose response curves plotted using Excel. All experiments  
were performed in triplicate and repeated three times.

The IC<sub>50</sub> values of copper(II) complex 4 for other cancer cell  
105 lines (cervical, ovarian, lung, NPC, breast, lymphoma leukemia  
and colorectal cancer) and four noncancer cell lines (kidney  
epithelial (HK-2), foreskin keratinocytes (HK-22, HK-398),  
nasopharyngeal epithelial (NP69)) were similarly obtained. After  
24 h drug exposure, 20 µL of Cell Titer 96® Aqueous One  
110 Solution Reagent (Promega) per well was added and the plate  
was incubated (37 °C, 5 % CO<sub>2</sub>) for a further 3 h. The absorbance  
at 490 nm was obtained by using a 96-well plate reader

(EnVision Multilable Plate Readers, PerkinElmer). Absorbance at 630 nm was used to subtract the background. Percentage of cell viability and IC<sub>50</sub> values were calculated by using the statistical software GraphPad Prism 5 (GraphPad software, Inc. San Diego, CA).

### Apoptosis and cell cycle analysis by flow cytometry

Cells were treated with 5 μM [Cu(phen)(aa)(H<sub>2</sub>O)]NO<sub>3</sub> and Cu(8OHQ)<sub>2</sub> in separate 60 mm petri dish for 24 h when cells confluency reached 70-80 %. Cells were also cultured without treatment as control. Apoptosis assay was performed using Annexin V-FITC Apoptosis Detection Kit II (BD Pharmingen™). Culture medium with suspension cells was collected and cells were washed with cold PBS. PBS was then collected. Cells were trypsinised with 1 mL accutase (Millipore) at 37 °C for 5 min to completely detach the cells. Accutase with suspension cells were collected and centrifuged at 1000 rpm for 5 min. The pellet was resuspended in 1X binding buffer. Cell count was performed and 1 x 10<sup>6</sup> cells/mL was prepared. 100 μL of the solution (1 x 10<sup>5</sup> cells) was transferred into a 12 x 75-mm, 5 mL polystyrene round bottom test tube (Becton, Dickson and company). 5 μL of FITC Annexin V and 5 μL PI was added. Cells were mixed gently and incubated for 15 min at room temperature (RT) in the dark. 400 μL of 1X binding buffer was added. The samples were filtered into labeled 12 x 75-mm, 5 mL polystyrene round bottom test tubes with cell strainer caps and analyzed immediately by fluorescent activated cell sorter (FACS-Calibur, Becton-Dickinson). Unstained cells, cells stained with Annexin V-FITC alone and cells stained with PI alone were used as control to set up compensation and quadrants. BD CellQuest Pro software was used to analyze the data.

Cells were exposed to 5 μM with [Cu(phen)(aa)(H<sub>2</sub>O)]NO<sub>3</sub> complexes for 24 h when cells grown to 70 % confluence in a 60 mm tissue culture dishes. Cells were cultured without treatment as control. Culture media with floating cells were collected and cells were washed with PBS. Cells were trypsinised with 1 mL accutase and then incubated at 37°C in a 5 % CO<sub>2</sub> incubator for 5 min until cells detached completely. Cells were collected, centrifuged for 5 min at 1000 rpm at RT and finally the pellets were resuspended in PBS. Cell count was performed by Countess® Automated Cell Counter. The concentration of cells was adjusted to 0.5-1.0 x 10<sup>6</sup> cells/mL and spun at 1000 rpm for 5 min. Supernatant was discarded and pellets was mixed well with 300 μL of hypotonic DNA staining buffer (0.25 g sodium citrate, 0.75 mL Triton™ X-100, 0.025 g propidium iodide, 0.005 g ribonuclease A and 250 mL distilled water). Each sample was filtered into a labeled 12 x 75-mm tube with cell strainer cap and kept at 4 °C protected from light for at least 10 min before analysis. The samples were mixed well and 20,000 cells were analyzed per sample by passage through a FACSCalibur employing the BD CellQuest Pro software. The percentage of cells in each phase of the cell cycle was analyzed using ModFit LT™ software (Verity Software House, Inc. ME).

### ROS assay

Treated or untreated MDA-MB-231 cells and MCF 10A cells at 70-80 % confluence were seeded at 0.5 x 10<sup>6</sup> in 6 cm culture plate and were treated with indicated concentration of [Cu(phen)(aa)(H<sub>2</sub>O)]NO<sub>3</sub> complexes and for different incubation time. The incubation time for one set treatment involving 5 μM and 10 μM copper(II) complexes was 6 h while that for another set involving 5 μM of same complexes was 24 h. Cells were rinsed with PBS. Then, trypsinization was performed by using accutase to detach cells and spun down at 1000 rpm for 5 min. Each pellet was suspended with 500 μL of 10 μM DCFH-DA (Sigma) solubilized in PBS and then incubated for 30 min at 37 °C in the dark. The cells were again spun down, the excess DCFH-DA was aspirated and the pellets were washed three times with PBS. Finally, the cells were suspended in PBS. The DCF fluorescence was measured immediately at 488 nm excitation and 525 nm emission (fluorescein isothiocyanate filter) using FACSCalibur with 20,000 events recorded. Data were analyzed by using BD CellQuest Pro software. The amount of ROS was quantified as the mean fluorescence intensity.

### γ-H2AX assay for DNA double strand breaks

MDA-MB-231 cells and MCF 10A cells were seeded in 2-well Lab-Tek II Chambered with cover glass slide (Nalge Nunc International) at a density of 1.2 x 10<sup>5</sup> cells/well and incubated overnight. Media were removed from the wells and the cells were treated with fresh media with 5 μM compounds for 6 h. Extra well was prepared for untreated cell and 1 μM adriamycin-treated cell. Adriamycin served as positive control. An isotype control is to confirm that the antibody H2AX binding is specific and not a result of non-specific binding of the fluorescent antibody.

After treatment, media were removed and cells washed with PBS. Cells were fixed with 3.7 % formaldehyde in PBS and incubated for 10 minutes at RT. Fixative was removed and the cells were washed twice with PBS. The cells were permeabilized by using 0.1 % Triton™ X-100 in PBS and incubated for 5 min at RT. The permeabilization buffer was removed and cells were washed twice with PBS. After Alexa Fluor® 488 Mouse anti-H2AX (pS139) was diluted at 1:10 ratio in 3 % BSA/PBS and added to each well. However, the isotype control (concentration as primary antibody) was added to untreated well and Adriamycin treated well. The cells were incubated for 60 min at RT in the dark. The antibody was removed and washed three times with 0.05 % Tween-20 in PBS. The nuclei were counterstain with 1 μg/mL solution of DAPI for 5 min. Slide was mounted using Vectasheild® mounting medium before imaging. Fluorescence images were captured using a Nikon microscope equipped with a CCD camera and NIS software. All the images were obtained using same parameters (exposure time and brightness) for direct comparisons and cell scoring analyzed by MetaMorp® microscopy automation and image analysis software.

### Proteasome inhibition

#### Chymotrypsin-like inhibition in 20S rabbit proteasome

The chymotrypsin-like activity of the proteasome was determined as previously described.<sup>14</sup> Briefly, a total volume of 50  $\mu$ L each assay mixture, consisting of 10  $\mu$ L purified 20S rabbit proteasome (0.10  $\mu$ g/well) with 10  $\mu$ L of 20  $\mu$ M fluorogenic peptide substrate, Suc-Leu-Leu-Val-Tyr-AMC, an appropriate volume of assay buffer (50 mM Tris-HCl, pH 7.5) and 25  $\mu$ L of each test compound at indicated concentration or 30  $\mu$ L of solvent as control in a 96-well fluorometer plate, was incubated for 30 min at 37°. After incubation, production of hydrolyzed fluorescent 7-amido-4-methyl-coumarin (AMC) groups was measured using an ELISA plate reader (Dynatech MRX) with an excitation filter of 380 nm and an emission filter of 460 nm. Chymotrypsin-like activity (%) was calculated as 100 x (Mean optical density of sample)/(Mean optical density of control). Changes in fluorescence were calculated against non-treated controls and plotted with statistical analysis using Microsoft Excel™ software.

#### Inhibition of proteolytic sites of 26S proteasome of MDA-MD-231 and MCF10A cells

The proteasome-Glo™ cell-based reagents were used to test the inhibition of complex **4** on the chymotrypsin-like, trypsin-like and caspase-like activities of 26S proteasome of MDA-MD-231 and MCF10A cells, according to the protocol of the supplier Promega. On adding singly each of the three luminogenic proteasome substrates (Suc-LLVY-aminoluciferin, Z-LRR-aminoluciferin and Z-nLPnLD-aminoluciferin) in optimised buffer to the viable cells, the proteasome substrate will be cleaved into its peptide and aminoluciferin components. Luciferase enzyme in the buffer then reacts with aminoluciferin to release light. Briefly, 2.5 x 10<sup>4</sup> MCF10 A cells or 1 x 10<sup>4</sup> MDA-MB-132 cells were plated on white 96-well plates. Cells were incubated with 6 or 10  $\mu$ M of **4** or 5  $\mu$ M of MG132 (positive control) for 6 h in a CO<sub>2</sub>-incubator at 37 °C. Then, each proteasome substrate was added into treated cells, resultant mixture was shaken at 760 rpm with a plate shaker for 2 min and then incubated for 10 min in the dark before measuring the luminescence a Panommics luminometer. Activity of each proteolytic site (%) was calculated as 100 x (Mean optical density of sample)/(Mean optical density of control). All experiments were performed in triplicate and repeated three times. The results are depicted as bar charts.

#### Whole cell extracts

MDA-MB-231 cells were treated with 5  $\mu$ M and 10  $\mu$ M of [Cu(phen)(aa)(H<sub>2</sub>O)]NO<sub>3</sub> complexes and Cu(8OHQ)<sub>2</sub> in petri dishes for 24 h. Cell extract preparation was from a previous published procedure.<sup>13</sup> After 24h, both floating and monolayer cells were harvested and lysated with lysis buffer (50 mM Tris-HCl, pH 8.0, 5 mM EDTA, 150 mM NaCl, 0.5 % Nonidet P-40, 0.5 mM phenylmethylsulfonyl fluoride, and 0.5 mM dithiothreitol) for 30 min at 4 °C. Afterwards, the lysates were centrifuged at 12,000 g for 30 min, and the supernatants were collected as whole cell extracts. Pellet was discarded. The supernatants containing proteins were known as whole cell extracts. Protein concentration was determined using biuret

method (BioRad). The supernatants were kept in ice until used for further analysis.

#### Western blot

The western blot analysis is a slight modification of a previous procedure.<sup>14</sup> Cell lysates (20 mg) were subjected to SDS-PAGE and then transferred to a polyvinylidene fluoride membrane, followed by visualization via the enhanced chemiluminescence (ECL) working solution of the SuperSignal West Pico Chemiluminescent Substrate (Thermo Scientific) or Western lighting™ Chemiluminescence Reagent Plus (PerkinElmer). The ECL Western blot analysis was performed using specific antibodies to Ubiquitin (P4D1) and I $\kappa$ B- $\alpha$  (C-15) and  $\beta$ -actin.

#### Statistical analysis

Statistical analysis was conducted using statistical software of GraphPad Prism 5 (GraphPad software, Inc. San Diego, CA). Differences between untreated and compound-treated samples were compared by one-way analysis of variance (ANOVA) with post hoc Dunnett's tests. Data were expressed as mean  $\pm$  S.E.M and for significant differences were set up at \* = p < 0.05, \*\* = p < 0.01, \*\*\* = p < 0.005.

## Results and discussion

### Chemistry

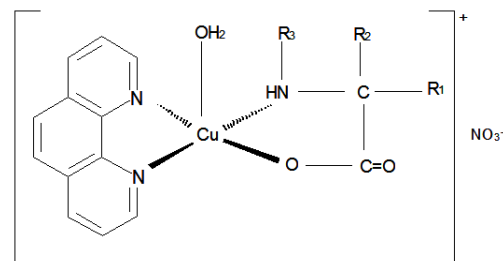


**Fig. 1** Structure of [Cu(phen)(aa)(H<sub>2</sub>O)]NO<sub>3</sub> (**1**: aa = gly, R<sub>1</sub>=R<sub>2</sub>=R<sub>3</sub>=H; **2**: aa = DL-ala, R<sub>1</sub>= CH<sub>3</sub>, R<sub>2</sub>=R<sub>3</sub>=H; **3**: aa = sar, R<sub>1</sub>=R<sub>2</sub>=H; R<sub>3</sub>= CH<sub>3</sub>; **4**: aa = C-dmg, R<sub>1</sub>= R<sub>2</sub>= CH<sub>3</sub>, R<sub>3</sub>= H)

X-ray crystal structure diffraction and other characterization data have established that each of the tested copper(II) complexes, **1-4**, have a square pyramidal [Cu(phen)(aa)(H<sub>2</sub>O)]<sup>+</sup> cation (Fig. 1) and an uncoordinated nitrate anion with or without lattice water molecule(s).<sup>19</sup> The amino acids, aa, are glycine and methylated glycine derivatives (alanine or 2-methylglycine; 2,2-dimethylglycine; sarcosine or N-methylglycine). In aqueous solution, they existed as 1:1 electrolyte and monitoring of their conductivity and visible spectra for 24 hours showed that they were stable. Positive-ion ESI-MS spectra showed only m/z peaks due to [Cu(phen)(aa)]<sup>+</sup> with the correct copper isotopic ratio, thus confirming the presence of the copper(II) complex cations in solution.<sup>19</sup> No copper(II) species arising from the dissociation of the coordinated amino acid was detected in each ESI-MS spectrum. In other words, the solid copper(II) complexes

dissolved in aqueous solution to yield the  $\text{NO}_3^-$ , and  $[\text{Cu}(\text{phen})(\text{aa})(\text{H}_2\text{O})]^+$ . The latter was stable at least up to 24 h.

#### Anticancer selectivity from morphology, MTT and apoptosis evidence

The morphological effects of treatment with varying concentration (1.6, 3.1, 6.3, 12.5, 25  $\mu\text{M}$ ) of the complexes **1-4** on human breast cancer MDA-MB-231 and non-malignant human breast epithelial MCF10A cells were examined and imaged for evidence of induced apoptosis. MDA-MB-231 cells (an oestrogen and progesterone receptor-negative cell line with mutant p53) are highly malignant, metastatic and invasive, whereas, MCF10A cells are non-invasive and lack of functional estrogen receptor and progesterone receptor. Both cell lines belong to the Basal B category.<sup>23,24</sup> MCF10A cells retain many of the characteristics of normal human cells.<sup>25</sup>

In the observation of morphological changes in carcinoma MDA-MB-231 cells, untreated cells maintained their morphology, appeared robust, elongated, adherent and showed cellular crowding, suggestive of normal proliferation. On the other hand, the morphology of cells was altered after treatment with **1-4**. The cells seemed to grow slower, losing their characteristic morphology, retracting and forming islets of more rounded cells with elevated concentrations of copper(II) complexes after 24 h of treatment (Fig. 2 as e.g.; Sup. Figs. 1.1-1.5 A & B). The characteristic morphological features of apoptotic cells are that cells are rounded and shrunken by cleavage of lamin and actin filaments in the cytoskeleton, nuclear condensation, membrane blebs and formation of apoptotic bodies.<sup>26,27</sup>

Cells of both cell types became altered in shape and lost their normal cellular morphology including cell size (diameter or area, shape and granularity) after treatment with **1-4** in a dose-dependent manner. However, concentration of these copper(II) complexes for initiation of morphological change varied between treated MDA-MB-231 and MCF10A cells. MDA-MB-231 cells treated with 3.1  $\mu\text{M}$  of all the copper(II) complexes showed obvious morphological change after 24 h (Sup Figs. 1.1A – 1.5A), while similarly treated MCF10A cells still maintained a normal morphology (Sup. Figs. 1.1B – 1.5B). Nevertheless, morphological changes could be observed at higher doses of copper(II) complexes in MCF10A. Apoptotic morphological changes such as shrunken cells and characteristic apoptotic blebbing were detected for MCF10A cells at 6.3 – 25  $\mu\text{M}$  of copper(II) complexes after 24 h of treatment. These results showed that copper(II) complexes **1-4** were all cytoselective towards the cancer cells at low concentration (3  $\mu\text{M}$ ). However, the known anticancer  $[\text{Cu}(\text{8OHQ})_2]$  induced morphological changes due to apoptosis in both MDA-MB-231 and MCF10A cells at low concentration (3.1  $\mu\text{M}$ ), suggesting its indiscriminate nature and severe toxicity to both cell lines.

For analyzing the antiproliferative effect of complexes **1-4** on cell viability, the tumorigenic human breast cancer cells (MDA-MB-231) and non-tumorigenic human breast epithelial cell line (MCF10A) were treated with increasing concentration of tested

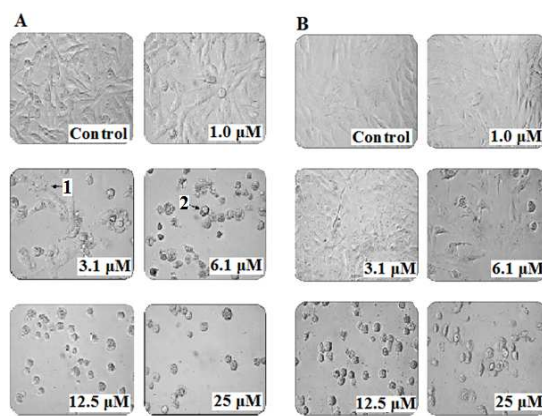


**Fig. 2** Morphological changes in MDA-MB-231 cells (A) and MCF10A (B) treated for 24 h with copper(II) complex **2** at different concentrations as compared to untreated cells. (Microscope magnification 400x). All pictures are typical of three independent experiments each performed under identical conditions. Arrows: (1) condensation of chromatin, (2) membrane bleb.

compounds (**1** – 25  $\mu\text{M}$ ) for 24 h. Figs. 3A-E show the dose response curves of the series of complexes **1-4** and  $[\text{Cu}(\text{8OHQ})_2]$  for both cell lines. MTT assay results showed these copper(II) complexes mediated dose-dependent decline in the viability of MDA-MB-231 and MCF 10A cell lines.

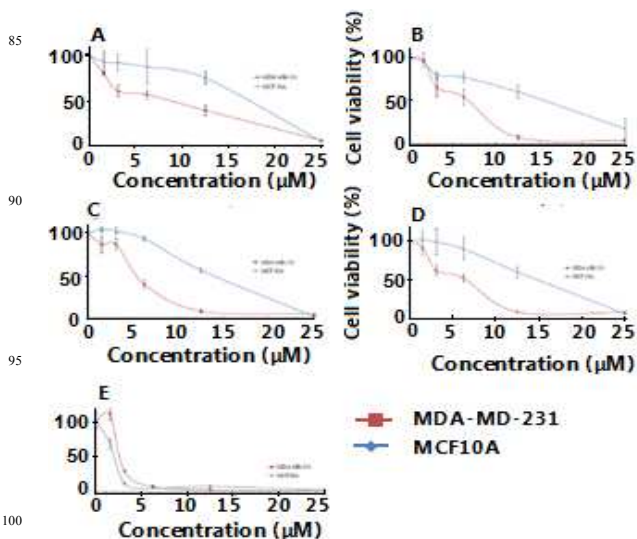


**Fig. 3** Dose response curve of the anti-proliferative activity (% cell viability) of copper(II) complexes **1** (A), **2** (B), **3** (C), **4** (D) and  $[\text{Cu}(\text{8OHQ})_2]$  (E) in MDA-MB-231 and MCF10A cells at 24 h. Cell viability is expressed as relative activity of control cells (100%). Results are the mean of at least three independent experiments and error bars show the standard error of the mean.

There was only a slight reduction in cell viability at 1.6  $\mu\text{M}$  compound-treated (**1-4**) MDA-MB-231 cells. After that, the cell viability decreased more sharply from 3.1 to 12.5  $\mu\text{M}$ . Inhibition of the cancer cell growth was greater than 90 % when cells were

1 treated with 25  $\mu\text{M}$  of every compound (Fig. 3A-E). Besides that,  
 2 the gaps between the dose response curves of both cell lines as  
 3 shown in the Fig. 3A-E were wider in the concentration range  
 4 6.25  $\mu\text{M}$  to 12.5  $\mu\text{M}$  for the complexes **1-4**, showing the more  
 5 pronounced rate of reduced proliferation for the cancer cells over  
 6 the normal cells.

7 Analysis of the above antiproliferative results for **1-4** is  
 8 described in detail here by using **3** as an example. For MDA-MB-  
 9 231 cells treated with **3**, the cell viability was 87 % when treated  
 10 with 3.1  $\mu\text{M}$  and decreased to approximately 10 % cell viability  
 11 at 12.5  $\mu\text{M}$  (Fig. 3B). In contrast, 98 % and 63 % cell viabilities  
 12 were observed when MCF 10A cells were treated respectively  
 13 with 3.1  $\mu\text{M}$  and 12.5  $\mu\text{M}$  of this copper(II) complex. Other  
 14 copper(II) complexes (**1**, **2**, **4**) produced similar results.  
 15 Therefore, complexes **1-4** are distinctly more antiproliferative  
 16 against MDA-MB-231 cancer cells than MCF10A normal cells,  
 17 i.e. they exhibit significant antiproliferative selectivity.

18 In contrast, the results of 24 h MTT assay revealed that  
 19  $[\text{Cu}(\text{8OHQ})_2]$  (known anticancer compound), equally inhibited  
 20 cell viability and decreased proliferation in both cell lines in a  
 21 dose-dependent manner. Cell viabilities for MDA-MB-231 cells  
 22 treated with 3.1  $\mu\text{M}$  and 6.3  $\mu\text{M}$  of  $[\text{Cu}(\text{8OHQ})_2]$  were 24 % and  
 23 4 % respectively while corresponding values for MCF10A treated  
 24 cells were 17 % and 3 % respectively (Fig. 3E). Anti-proliferative  
 25 results collaborated the earlier morphological changes which  
 26 occurred when cells of both cell lines were treated with  
 27 increasing concentration of the copper(II) complexes. Therefore,  
 28  $[\text{Cu}(\text{8OHQ})_2]$  is not antiproliferatively selective.

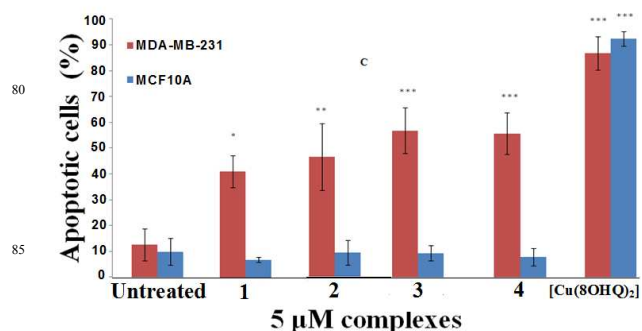
29 **Table 1**  $\text{IC}_{50}$  values ( $\mu\text{M}$ ) for proliferation inhibition by  
 30 copper(II) complexes **1-4** and  $[\text{Cu}(\text{8OHQ})_2]$  for 24 h treatment.  
 31  $\text{IC}_{50}$  values were calculated from dose-response curves. Data are  
 32 mean  $\pm$  S. D.

Compounds	$\text{IC}_{50}$ ( $\mu\text{M}$ )		Therapeutic Index
	MDA-MB-231	MCF10A	
<b>1</b>	$8.5 \pm 0.3$	$15.8 \pm 0.6$	1.9
<b>2</b>	$5.2 \pm 0.2$	$16.5 \pm 2.3$	3.2
<b>3</b>	$5.5 \pm 1.1$	$13.9 \pm 2.1$	2.5
<b>4</b>	$6.2 \pm 1.1$	$15.1 \pm 1.6$	2.4
$[\text{Cu}(\text{8OHQ})_2]$	$2.7 \pm 0.2$	$1.6 \pm 0.4$	0.6

33 The antiproliferative property of each compound was also  
 34 determined in the form of  $\text{IC}_{50}$  concentration (50 % growth  
 35 inhibitory concentration) from Fig. 3A-E. The  $\text{IC}_{50}$  data of all the  
 36 compounds are tabulated (Table 1). Interestingly,  $\text{IC}_{50}$  of **1** in  
 37 MDA-MB-231 cell was  $8.5 \pm 0.3$   $\mu\text{M}$  and those for all the  
 38 copper(II) compounds with methylated glycine derivatives (**2-4**)  
 39 were  $5.5 \pm 1.1$   $\mu\text{M}$ ,  $5.2 \pm 0.2$   $\mu\text{M}$  and  $6.2 \pm 1.1$   $\mu\text{M}$ , respectively.  
 40 All the complexes **1-4** were much more effective (by about 10x)  
 41 against MDA-MB-231 than cisplatin ( $\text{IC}_{50} = 63\text{-}66$   $\mu\text{M}$ ; 24  
 42 h).<sup>28,29</sup> The copper(II) complexes with coordinated methylated  
 43 glycine derivatives (**2-4**) had slightly lower  $\text{IC}_{50}$  values for MDA-  
 44 MB-231 compared to the corresponding complex with glycine  
 45 (**1**). However, the  $\text{IC}_{50}$  values of **1-4** for MCF10A ranged from

14-17  $\mu\text{M}$  and were significantly higher than those for MDA-  
 50 MB-231 (5-9  $\mu\text{M}$ ). Again analysis of  $\text{IC}_{50}$  values shows that these  
 copper(II) complexes were more antiproliferative towards cancer  
 cells than normal cells.

On the other hand, the  $\text{IC}_{50}$  value for the MCF10A treated  
 with  $[\text{Cu}(\text{8OHQ})_2]$  was  $1.6 \pm 0.4$   $\mu\text{M}$  which was lower than that  
 55 for MDA-MB-231 ( $2.7 \pm 0.2$   $\mu\text{M}$ ).  $[\text{Cu}(\text{8OHQ})_2]$  was slightly  
 more antiproliferative towards normal MCF10A cells rather than  
 cancerous MDA-MB-231 cells. To quantitatively compare the  
 selectivity of these complexes, their therapeutic indices (TI) [TI =  
 $\text{IC}_{50}(\text{MCF10A})/\text{IC}_{50}(\text{MDA-MB-231})$ ] can be calculated and these  
 60 are shown in Table 1.<sup>30</sup> TI with a value greater than 1 shows  
 selectivity and the higher the TI value, the higher the selectivity.  
 Thus, all the complexes **1-4** are more selective (TI, ~2-3x)  
 towards the cancer cells over the normal cells while  
 $[\text{Cu}(\text{8OHQ})_2]$  (TI, 0.6) is not. The selectivity is statistically  
 65 significant. The therapeutic indices of the complexes **1-4** are  
 comparable to those of PI-083, a selective inhibitor against  
 proteasomal chymotrypsin-like activity which was discovered by  
 screening compounds in the NCI chemical libraries.<sup>13</sup> We have  
 calculated the TI values (24 h incubation) of PI-083 for ovary cell  
 70 lines (T80 vs T80-Hras), pancreas cell lines (C7 vs C7-Kras),  
 and breast cell lines (MCF10A vs MCF-7) to be 1.8, 2.1 and 3.8.  
 In the same report, bortezomib was found to be not selective. In  
 fact, we also found that complexes **1-4** were also more effective  
 against tumorigenic nasopharyngeal cell line (HK1) than  
 75 corresponding non-tumorigenic cell line (NP69) with higher TI  
 values.<sup>19</sup>



37 **Fig. 4** Percentage of apoptotic cells after treatment with 5  $\mu\text{M}$   
 38 copper(II) complexes **1-4** and  $[\text{Cu}(\text{8OHQ})_2]$  at 24h in MDA-  
 39 MB-231 and MCF10A cell lines. Results are the mean of three  
 40 independent experiments and error bars show the standard error  
 41 of the mean. \* = ( $p < 0.05$ ), \*\* = ( $p < 0.01$ ), \*\*\* = ( $p < 0.005$ )  
 42 indicates significantly different from untreated.

43 To check whether inhibition of proliferation by the above  
 44 four complexes (**1-4**) involved apoptosis, flow cytometric  
 45 analysis of apoptosis was done. Very low percentage of apoptotic  
 46 cells were detected in both untreated MDA-MB-231 and  
 47 MCF10A cells, demonstrating normal cell viability (Fig. 4).  
 48 Treatment of MDA-MB-231 cells with 5  $\mu\text{M}$  **1**, **2**, **3** and **4**  
 49 resulted in 41.14 %, 46.33 %, 56.84 % and 55.64 % apoptotic  
 50 cells respectively (Fig. 4; Sup. Figs. 2.1-2.2). Further analysis of  
 flow cytometric data clearly showed treatment with complexes **1-**

4 induced apoptotic cell death more than fourfold relative to untreated for MDA-MB-231 cells. On the contrary, the percentage of apoptotic cells for compound-treated MCF10A ranged from 7 to 10 %, which were comparable to that found for untreated cells, showing MCF10A cells were unaffected by 5  $\mu\text{M}$  of these copper(II) complexes (Fig. 4). This selective apoptosis-inducing property is good reason for further detailed testing and evaluation of the above series of complexes as anticancer drug in animal model is in progress.

In contrast,  $[\text{Cu}(\text{8OHQ})_2]$  induced approximately 90 % apoptotic cell death in both cell lines (Fig. 4). As depicted in Sup Figs. 2.1-2.2, 90.21 % MDA-MB-231 cells treated with 5  $\mu\text{M}$   $[\text{Cu}(\text{8OHQ})_2]$  became apoptotic and 94.64 % of similarly treated MCF10A became apoptotic.  $[\text{Cu}(\text{8OHQ})_2]$  exhibited similar high cytotoxicity towards both cell lines. It's induction of apoptosis is therefore indiscriminate or non-cytoselective. It is unclear why this is so.

### Anticancer selectivity and ROS levels

Jungwirth *et al* has recently reviewed the role of redox processes in anticancer metal complexes, including those of copper.<sup>3</sup> In fact, copper complexes are well known for their redox properties and generation of ROS. However, most studies involve only cell-free systems.<sup>3</sup> To investigate the possible generation of ROS in breast cells (MDA-MB-231 and MCF10A) by complexes 1-4, both cell lines were treated with indicated concentration of copper(II) complexes (5  $\mu\text{M}$ , 10  $\mu\text{M}$ ) and at different incubation time (6 h, 24 h). The intracellular ROS levels were detected by flow cytometric analysis using the fluorophore, dichlorofluorescein diacetate (DCFH-DA) which is a well-established compound to detect and quantify intracellular ROS ( $\text{H}_2\text{O}_2$ ,  $\cdot\text{OH}$ ).<sup>31,32</sup> Increase in dichlorofluorescein (DCF) fluorescence will reflect increase in oxidation of non-fluorescent dichlorofluorescein (DCFH) to DCF, indicating higher ROS level.

The choice of the 6h incubation time was because live cell imaging study using microscopy technique showed that complexes 1-4 were able to induce morphology changes (diameter, shape and granularity) in MDA-MB-231 cells, indicative of onset of apoptosis (data not shown). Based on this finding, 6 h had been selected for ROS study (and the subsequent  $\gamma\text{-H2AX}$  assay to detect cellular DNA damage).

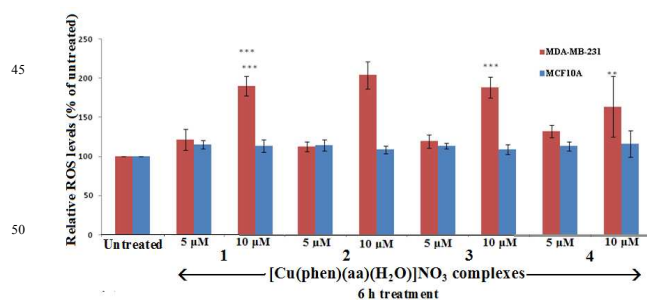


**Fig. 5** ROS production induced by copper(II) complexes 1 – 4 treatment with different concentration for 6 h. The average of data obtained in three independent experiments. Results are mean  $\pm$  S.D. (n=3).

The exposure of the MDA-MB-231 and MCF10A to any of the 1-4 complexes at 5  $\mu\text{M}$  for 6 h resulted in insignificant increase in relative fluorescence compared to untreated cells (Fig. 5). However, exposure of MDA-MB-231 cells to 10  $\mu\text{M}$  of 1-4 for 6 h led to significant increase in ROS production compared to untreated cells, as shown in Fig. 5. On the other hand, 10  $\mu\text{M}$  of these copper(II) complexes still had no effect on the ROS levels in MCF10A treated cells as there is no statistically significant increase in ROS compared to untreated cells (Fig. 5). This suggests there is a safe minimum dosage of copper(II) complexes to induce significant ROS increase in cancer cells without altering the ROS levels in normal cells.

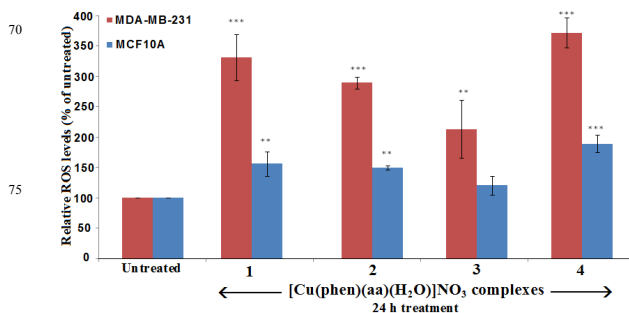


**Fig. 6** ROS production induced by 5  $\mu\text{M}$  copper(II) complexes 1 – 4 treatment for 24 h. The average of data obtained in three independent experiments. Results are mean  $\pm$  S.D. (n=3).

For 24 h treatment, strong DCF fluorescence of up to 3-fold was observed in 5  $\mu\text{M}$  compound-treated MDA-MB-231 cells (Fig. 6). Although the production of ROS in 5  $\mu\text{M}$  copper(II) complex-treated MCF10A cells (except complex 3) is statistically significant after 24 h incubation, the increase in ROS in MCF10A was appreciably lower than that in MDA-MB-231 cells. Collectively, these data imply that ROS production in these copper(II) complexes-treated cells was concentration- and time-dependent manner in MDA-MB-231 cell line. Clearly, it is feasible to alter concentration of copper(II) complexes and incubation time to generate significantly higher ROS in cancer cells compared to untreated cancer cells without affecting ROS levels in normal cells or merely raising ROS levels to non-dangerous levels.

In fact, a combination of N-acetylcysteine (NC; a thiol) and  $\text{CuCl}_2$  was able to selectively generate cytotoxic ROS and induce apoptosis in MCF7 cancer cells.<sup>33</sup> MCF 10A was insensitive to NC/Cu(II) treatment. Similar findings were also reported for (-)-Epigallocatechin-3-gallate which was found to induce apoptosis in cancer cells without adversely affecting normal cells, and the selectivity arose from differential induction of ROS and consequent differential modulation of expression of apoptosis-related genes in both types of cells.<sup>34</sup> At least for 24 h incubation, greater antiproliferative inhibition of cell growth and more killing of cancer cells by 10  $\mu\text{M}$  copper(II) complexes 1 - 4 compared to normal cells may be due to the higher ROS generated in cancer

cells than in normal cells. This result therefore supports the strategy for use of copper(II) complexes to selectively kill cancer cells, and their further development for selective anticancer therapy. However, it is still unclear why some copper(II) complexes, for example the currently tested neutral  $[\text{Cu}(\text{8OHQ})_2]$  and a previously reported ionic  $[\text{Cu}(\text{phen})_3](\text{ClO}_4)_2$  complex (phenanthroline = 1,10-phenanthroline-5,6-dione), were not cytoselective.<sup>35</sup>

The greater sensitivity of cancer cells to killing by some copper(II) complexes may involve cellular redox homeostasis and the presumed existence in both types of cells a common minimum ROS threshold level at which its attainment initiates apoptosis.<sup>5</sup> Many types of cancer cells have higher basal ROS and decreased antioxidants. The greater generation of ROS in MDA-MB-231 cancer cells than in MCF10A normal cells could easily push the ROS level to reach the ROS threshold without adequate antioxidants, and thus preferentially initiate apoptosis in the former.

Complex **4** was chosen as a representative to find out whether ROS-induced loss in viability of MDA-MB-231 can be rescued, and this was done by pretreating cells with NAC for 1 h before treating these cells with **4** for 24 h.<sup>8</sup> Chaudhuri *et al* found that pretreatment of doxorubicin resistant T. Lymphoblastic leukemia cells with the antioxidant NAC could completely block ROS generation and abrogated apoptosis induced by copper(II) complex of N-(2-hydroxyacetophenone)glycinate.<sup>8</sup> Surprisingly, the NAC (0.01-2.50 mM) did not rescue the MDA-MB-231 cells treated with 6 or 10  $\mu\text{M}$  of **4** and there was no significant change in their viability compared with control cells (Fig. 7). Whether ROS induced by **4** is quenchable by other ROS-specific antioxidants and whether the ROS-induced apoptosis by **4** can be rescued or abrogated needs further investigation.

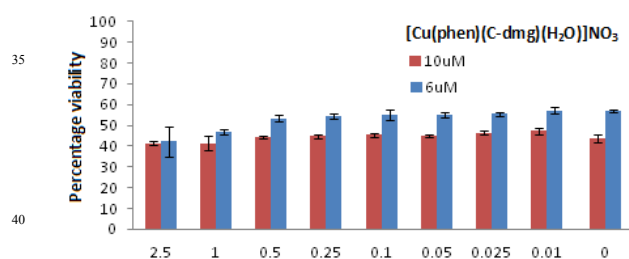


**Fig. 7** Effect of pretreatment of MDA-MB-231 cells with antioxidant NAC for 1 h prior to further incubation with **4** for 24 h. Media with NAC were removed before adding fresh media and **4**.

### Selective cell cycle arrest

In the earlier section, we established that decreased cell viability of MDA-MB-231 cells was due to apoptosis. To determine the effects of complexes **1-4** on cell cycle distribution, MDA-MB-231 and MCF10A cells were treated with 5  $\mu\text{M}$  of these copper(II) complexes for 24 h and analyzed by flow cytometry. The percentage of cells in each phase of the cell cycle was

determined by using *Modfit* LT software (*Verity* Software House, Topsham, ME).

The distribution of cells in three major phases of the cell cycle ( $G_0/G_1$ , S,  $G_2/M$ ) in DNA histograms of MDA-MB-231 cells and MCF10A cells after 24 h of treatment with 5  $\mu\text{M}$  copper(II) complexes are shown in Figs. 8 - 9. Fig. 8 illustrates that the average percentage of cells in different phases for MDA-MB-231 cells treated with complexes **1-4** were compared with those of untreated cells. As depicted in Fig. 8,  $G_0/G_1$ , S phase and  $G_2/M$  of untreated MDA-MB-231 cells were 56.28 %  $\pm$  2.5 (mean  $\pm$  SD), 33.98 %  $\pm$  2.5 and 9.73 %  $\pm$  0.2 respectively. For MDA-MB-231 cells treated with **2**, the percentage of cell population at  $G_0/G_1$  phase increased to 69.34 %  $\pm$  2.7 but those at S phase and  $G_2/M$  decreased to 26.06 %  $\pm$  3.1 and 4.6 %  $\pm$  0.4 respectively. Statistical analysis ( $p < 0.05$ ) showed that the increases in  $G_0/G_1$  phase for **2** and **4** were significant. This indicates that these two complexes induced cell cycle arrest at  $G_0/G_1$  (Sup Table 1) and the methyl substituent at the  $\alpha$ -carbon of the amino acid may be important. This cell cycle arrest at  $G_0/G_1$  is often the result of respective cell cycle checkpoint activation due to DNA damage.<sup>37</sup> On the other hand, cisplatin and oxaplatin are known to induce cell cycle arrest at S phase which signifies inhibition of DNA synthesis.<sup>38,39</sup> Such difference in type of phase-arrest implies different mechanistic pathway. Treatment with other copper(II) complexes (**1**, **3**) resulted in a rise in the percentage of cells in  $G_0/G_1$  with a concomitant decrease in the percentage S phase and  $G_2/M$  phase in MDA-MB-231 but the increases were not statistically significant (Sup Table 1).

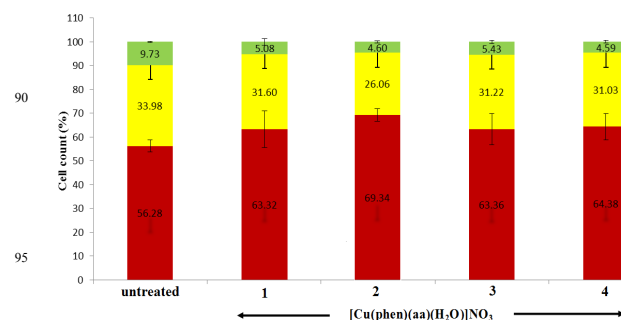


**Fig. 8** Cell cycle distribution of MDA-MB-231 cells in the absence or presence of 5  $\mu\text{M}$  copper(II) complexes **1-4** at 24 h. Data are presented as means of the percentage of cells in  $G_0/G_1$  (red), S (yellow) or  $G_2/M$  (green) phase from three independent experiments with S.D.

The results for the immortalized breast cell line, MCF10A, were different. The percentage of cells in  $G_0/G_1$ , S and  $G_2/M$  phases for cells treated with 5  $\mu\text{M}$  complexes **1-4** were comparable to those for untreated cells (Fig. 9). Thus, these copper(II) complexes did not affect the cell cycle of MCF10A cells, i.e. there was no cell cycle arrest, for 24 h incubation.

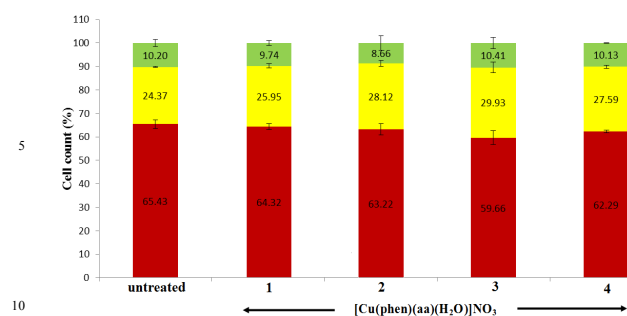
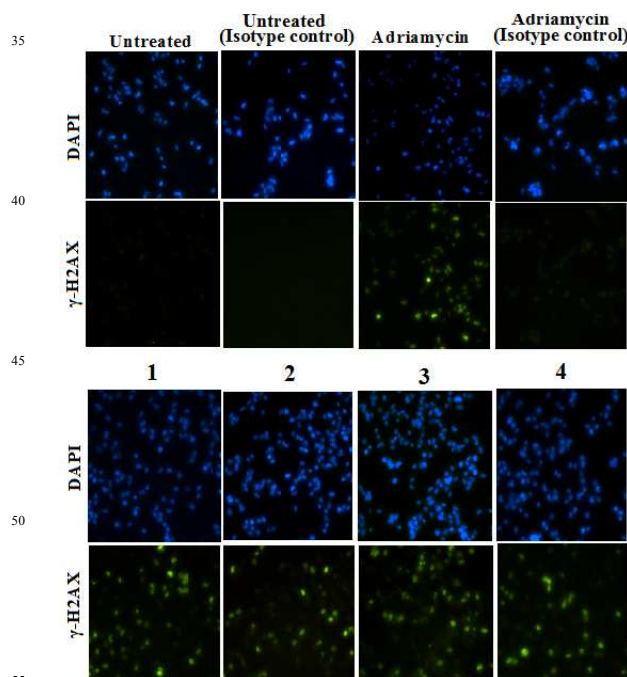


**Fig. 9** Cell cycle distribution of MCF10A cells in the absence or presence of 5  $\mu$ M copper(II) complexes **1** – **4** at 24 h. Data are presented as means of the percentage of cells in G<sub>0</sub>/G<sub>1</sub> (red), S (yellow) or G<sub>2</sub>/M (green) phase from three independent experiments with S.D.

### Selective intracellular DNA damage

It is well known that copper(II) and other redox active metal complexes could generate ROS under aerobic conditions or in the presence of oxidizing or reducing agents.<sup>3,36,40-42</sup> Published data demonstrated that copper(II) complexes can be used as metallodrugs to cause DNA damage and lead to decrease cell viability, cell cycle arrest and apoptotic cell death.<sup>43-45</sup> It is, therefore important to identify DNA as one of the targets for copper(II) complexes **1-4**. Intracellular DNA damage that lead to formation of DNA double strand breaks (DSBs) will induce phosphorylated H2AX on Ser<sup>139</sup> (denoted as  $\gamma$ -H2AX).<sup>46,47</sup> The  $\gamma$ -H2AX provides a marker of DSBs.<sup>48</sup> Therefore, histone  $\gamma$ -H2AX phosphorylation on Ser<sup>139</sup> assay was used to investigate DNA DSBs induced by these copper(II) complexes in MDA-MB-231 and MCF10A.



**Figs. 10** Immunofluorescence staining for  $\gamma$ -H2AX (green) in MDA-MB-231 cells after 6 h treatment with 5  $\mu$ M copper(II) complexes **1** - **4** compared to control cells. DNA counterstaining is with DAPI (blue). Results are representative of three independent experiments.

Isotype control used in the study was to act as a negative control, to exclude non-specific binding/background fluorescence. Adriamycin, as positive control, could induce  $\gamma$ -H2AX which can be detected in both MDA-MB-231 and MCF10A cells incubated with Alexa Fluor<sup>®</sup> 488-tagged specific antibodies against  $\gamma$ -H2AX by immunofluorescence staining and fluorescence microscopy (Figs. 10 - 11). For image analysis, three images were taken, *viz.* DAPI (4', 6-diamidino-2-phenylindole) channel, FITC channel and phase contrast. DAPI was used for DNA staining and DAPI specifically stains nuclei.

The  $\gamma$ -H2AX fluorescence (green) was significantly elevated in each individual copper(II) complex-treated MDA-MB-231 cells (Fig. 10). These results suggest 5  $\mu$ M copper(II) complexes induced DSBs quite early (6 h after administration) in cancer cells. One of the substrate phosphorylated by ataxia telangiectasia mutated (ATM) is histone H2AX, and the expression of  $\gamma$ -H2AX is mediated by ATM. Once ATM is activated, it leads to the downstream events such as recruitment of DNA repair machinery, engagement of cell cycle checkpoints, and activation of apoptotic pathway.<sup>49</sup> Accordingly, the results suggest that the treatment (6 h) with copper(II) complexes induced oxidative DNA damage and induced formation of  $\gamma$ -H2AX and lead to downstream apoptosis pathway. The cell scoring for the amount of  $\gamma$ -H2AX was also performed by using Metamorp<sup>®</sup> software. These data showed that the number of MDA-MB-231 cells stained positive for  $\gamma$ -H2AX induced by complexes **1-4** were statistically higher compared to untreated cells (Fig. 12).

Interestingly, a negative response for the  $\gamma$ -H2AX was observed after treatment of MCF10A with 5  $\mu$ M complexes **1-4** under the same condition (Fig. 11). This difference may be because MCF10A cells have enough antioxidants to prevent DNA damage by ROS at that particular copper(II) complex concentration and time point. In other words, sufficiently low concentration of **1-4** did not cause DSBs in MCF10A cells. In conclusion, **1-4** induced selective DNA damage in MDA-MB-231 cells without harming DNA of the MCF10A cells. This provides us sufficient basis to initiate investigation into the complex relationship involving ROS, cellular redox systems and apoptosis induction to further understand the selective redox control and execution of apoptosis by **1-4** in cancer and normal cells.<sup>50</sup>

### Proteasome inhibition

The human 26S proteasome is a large multicatalytic protease complex composed of two terminal 19S regulatory caps and a 20S proteolytic core with three different proteolytic sites.<sup>11,51</sup> One of these proteolytic sites has chymotrypsin-like activity and its inhibition is commonly tested for copper(II) complexes.<sup>14-17</sup> It has also been shown that proteasomal chymotrypsin-like inhibition is a strong apoptosis stimulus.<sup>15</sup> Inhibition of chymotrypsin-like

activity was tested on commercial 20S rabbit proteasome while inhibition of 26S proteasome was evaluated using MDA-MB-231 cell extract or live cells. 20S proteasome was incubated with increasing concentration of complexes 1-4, [Cu(8OHQ)<sub>2</sub>] and epoxomicin (as positive control) for 30 minutes.

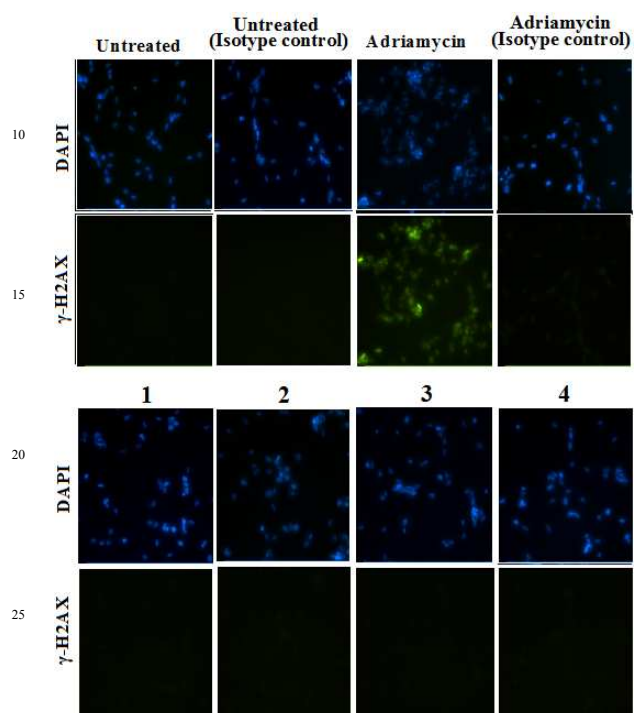


**Fig. 11** Immunofluorescence staining for  $\gamma$ -H2AX (green) in MCF10A cells after 6 h treatment with 5  $\mu$ M copper(II) complexes 1 - 4 compared to control cells. DNA counterstaining is with DAPI (blue). Results are representative of three independent experiments.

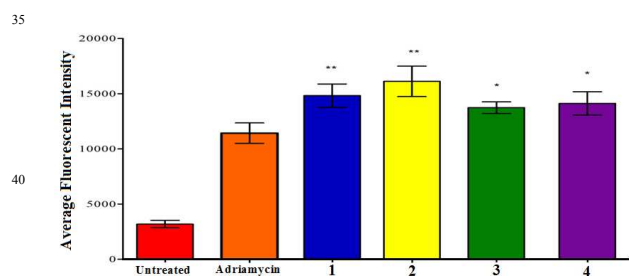


**Fig. 12** Cell intensity of  $\gamma$ H2AX production induced by copper(II) complexes in MDA-MB-231 cells. Results are mean  $\pm$  S.E.M.

[Cu(8OHQ)<sub>2</sub>] and epoxomicin were found to be good inhibitors of chymotrypsin-like activity (CT-L) of 20S proteasome with about 70% and 100% inhibition at 5  $\mu$ M (Fig. 13). Epoxomicin is a potent proteasome inhibitor which acts primarily inhibiting the chymotrypsin-like activity.<sup>52</sup> Bortezomid and carfilzomid are also potent inhibitors of this CT-L, and the inhibition was established to be due to each inhibitor forming covalent bond between its  $\alpha'$ , $\beta'$ -epoxy ketone pharmacore with

the amino terminal catalytic threonine-1 (THR-1) residue of  $\beta$ 5 subunit of the 20S proteasome.<sup>11</sup> Carfilzomid, discovered *via* a medicinal chemistry approach, is derived from epoxomicin.<sup>52</sup> However, copper(II) complexes 1-4 were poorer inhibitors of CT-L with less than 50% inhibition at the same concentration (5  $\mu$ M) of tested compounds. It is likely that the complexes 1-4 are weaker inhibitors of chymotrypsin-like activity of the  $\beta$ 5 active site due to weaker or non-covalent interaction of these complexes with the catalytic THR-1 which is used as a nucleophile to attack the carbonyl of the peptide bond destined for cleavage.

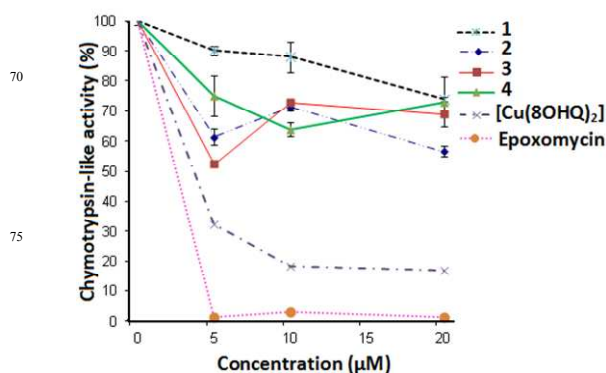


**Fig. 13** Inhibition of chymotrypsin-like activity of 20S rabbit proteasome by various copper(II) complexes and epoxomicin.

Next, we chose 4 to test for inhibition of chymotrypsin-like, trypsin-like and caspase-like proteolytic activities of 26S proteasome of intact MDA-MB-231 and MCF10A cells using a Proteasome Glo<sup>TM</sup> cell-based assay.<sup>53</sup> Different series of cells were incubated with test compounds for 6 h, followed by addition of the luminogenic proteasome substrate individually. The control MG132 (N-(benzyloxycarbonyl)leucylleucylleucinal or Z-Leu-Leu-Leu-al; a known proteasome inhibitor), at 5  $\mu$ M, almost totally inhibited all three sites (Fig. 14). Surprisingly, 6 and 10  $\mu$ M of 4 did not inhibit these three proteolytic sites of both types of cells, indicating no inhibition in terms of these three proteolytic sites. In all these cases, the treated cancer and normal cells were viable (data not shown). Six hours of incubation of live MDA-MD-231 cells with 6 or 10  $\mu$ M of 4 did not result in inhibition of chymotrypsin-like activity of cellular 26S proteasome but 30 minutes of incubation of isolated 20S proteasome with 5 or 10  $\mu$ M resulted in this inhibition. Other copper(II) complexes could inhibit this proteolytic site of 26S proteasome of cancer cell extracts for merely 2 h incubation.<sup>16,17</sup> Further research on this discrepancy is in progress.

If proteasome inhibition does not involve the three proteolytic sites of the 20S proteasome, it could involve the 19S regulatory cap of the 26S proteasome or the ubiquitination step. We proceeded to look at inhibition of degradation of ubiquitinated proteins by 1-4 in MDA-MB-231 cell extracts which contain 26S proteasome (Fig. 15). MDA-MB-231 cell extracts were treated with 1  $\mu$ M and 10  $\mu$ M of each of the above five copper(II) complexes for 24 h, followed by Western blotting using specific antibodies to ubiquitin, I $\kappa$ B- $\alpha$  and  $\beta$ -actin (a loading control).

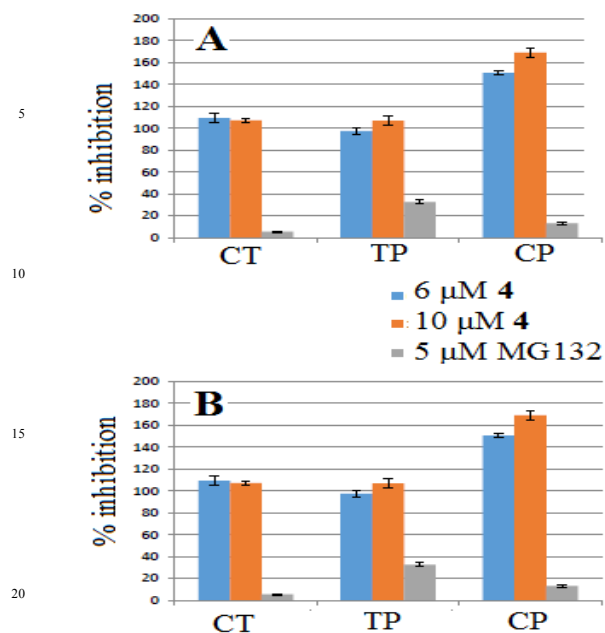


**Fig. 14 (A, B)** Inhibition of chymotrypsin-like(CT), trypsin-like(TP) and caspase-like(CP) activities of 26S proteasome of intact MDA-MB-231 (A) and MCF10A cells incubated with **4** for 6 h.

For untreated cells and those treated with 1 μM of all copper(II) complexes, western blot analysis showed similar low intensity of ubiquitinated proteins, suggesting no proteasomal inhibition. The greater intensity band in lane 11 (Fig. 15) indicates that 10 μM [Cu(8OHQ)<sub>2</sub>] could efficiently inhibit proteasome in MDA-MB-231 cells, in agreement with similar reported results.<sup>14,15</sup> Similarly, it was found that higher intensity and greater accumulation of ubiquitinated proteins occurred when cells were treated with higher concentration (10 μM) for all complexes **1-4**. The levels of ubiquitinated proteins for 10 μM [Cu(phen)(aa)(H<sub>2</sub>O)]NO<sub>3</sub>-treated (**1-4**) MDA-MB-231 cells were comparable to those for [Cu(8OHQ)<sub>2</sub>], a known 26S proteasome inhibitor.<sup>14</sup> This suggests that the inhibitor strength of **1-4** for 26S proteasome are similar to that of Cu(8OHQ)<sub>2</sub> although there was a vast difference in their ability to inhibit chymotrypsin-like activity in 20S rabbit proteasome. As **1-4** are weaker inhibitors of chymotrypsin-like activity, their high potency as proteasome inhibitors in cancer cells need to involve inhibition of some other relevant part of the 26S proteasome. Numerous reported anticancer copper(II) compounds are good inhibitors of the chymotrypsin-like activity of proteasome.<sup>17,54</sup> Recently, it was revealed that a copper(II) complex of diethyldithiocarbamate was more active against 26S proteasome than 20S proteasome, and it was postulated, without evidence, that it was due to inhibition of the 19S in the 26S proteasome.<sup>55</sup> However, a peptoid inhibitor of the proteasome 19S regulatory particle has been identified and it functions *via* inhibiting protein unfolding mediated by this 19S.<sup>56</sup>

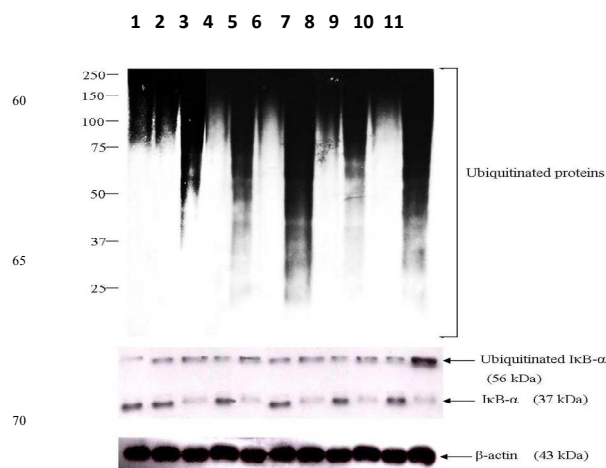


**Fig. 15** Western blot analysis for ubiquitinated protein and IκB expression (20 μg of total protein lysate/lane) obtained from human breast cancer MDA-MB-231 cells, treated with 5 μM of copper(II) complexes **1-4** for 24 h. β-actin was used as the loading control. The experiment was repeated three times with similar results. Lane 1, untreated; Lane 2, 1 μM of **2**; Lane 3, 10 μM of **2**; Lane 4, 1 μM of **3**; Lane 5, 10 μM of **3**; Lane 6: 1 μM of **1**; Lane 7, 10 μM of **1**; Lane 8, 1 μM of **4**; Lane 9, 10 μM of **4**; Lane 10, 1 μM of [Cu(8OHQ)<sub>2</sub>]; Lane 11, 10 μM of [Cu(8OHQ)<sub>2</sub>].

It is known that NF-κB (nuclear factor κB) is involved in growth and anti-apoptosis in normal and cancer cells.<sup>57</sup> Inactive forms NF-κB are bound to inhibitor IκB in the cytoplasm and is prevented from translocation into the nucleus. NF-κB activation is regulated by phosphorylation of IκB which results in its ubiquitination and its subsequent degradation by proteasome. Proteasome inhibitor functions to block the degradation of ubiquitinated IκB-α (56 kDa). Functional proteasome will cause degradation of the ubiquitinated IκB-α to smaller fragmented IκB-α (37 kDa) (Fig. 15 untreated control, lane 1). Extract from cancer cells treated with 1 μM of all five copper(II) complexes showed pattern of IκB-α bands similar to that from untreated cells, suggesting no inhibition of proteasome (Fig. 15: lanes 2, 4, 6, 8, 10). However, extraction from MDA-MB-231 cells treated with 10 μM of [Cu(8OHQ)<sub>2</sub>] showed an intense band of ubiquitinated IκB-α (56 kDa) and a faint band of degraded IκB-α (37 kDa), suggesting no degradation of the IκB-α (56 kDa) due to the proteasomal inhibition induced by [Cu(8OHQ)<sub>2</sub>] (Fig. 15, lane 11). In the experiment, the intensities of protein level of ubiquitinated IκB-α (56 kDa) and degraded IκB-α (37 kDa) for 10 μM [Cu(phen)(aa)(H<sub>2</sub>O)]NO<sub>3</sub>-treated cancer cells were similar to those of 10 μM [Cu(8OHQ)<sub>2</sub>]-treated cells. This indicates that 10 μM of [Cu(phen)(aa)(H<sub>2</sub>O)]NO<sub>3</sub> complexes (**1-4**) could also inhibit proteasome. Taken together, the above data suggest that the proteasome is a target of complexes **1-4** in MDA-MB-231 breast tumour cells and this inhibition contribute to their anticancer property. Since the results of the preceding

investigation using the Proteasome Glo™ cell-based assay showed that the three proteolytic sites of the 20S proteasome core are not involved, the western blot analysis results of ubiquitinated proteins suggests some unknown mechanism of inhibition of MDA-MD-231 26S proteasome. Further investigation is in progress to (i) monitor inhibition of the three proteolytic sites in the 26S proteasome of MDA-MD-231 and MCF10A cells treated with **4** over different incubation time, and (ii) to establish the role of 19S regulatory particles. We are also keen to establish whether inhibition of 19S leads to apoptosis and whether it can account for anticancer selectivity observed in our studies. Nevertheless, many types of cancer were more sensitive to proteasome inhibition.<sup>9,11</sup> This differential sensitivity may be related to a recent finding that proteasome activity was significantly elevated in advance stage of rectal, gastric and breast cancer of patients compared to that in normal individuals.<sup>11,58</sup>

### Effectiveness against a wide range of cancer types

Anticancer drugs are sometimes cancer-type specific. This factor and developed cell resistance limit the widespread use of such drugs. To address this issue, we tested the antiproliferative property of **4** on a wide variety of cancer cell lines of different tissue origin for 24 h incubation. It was found to be effective against cervical (Hela), ovarian (SKOV3), lung (A549, PC9), NPC (Hone1, HK1, C666-1), breast (MCF7, T47D), lymphoma leukemia (Nalmawa, HL60) and colorectal (SW480, SW48, HCT118) cancer cell lines with IC<sub>50</sub> values (24 h) in the 1.7 – 19.0 μM range (Fig. 16 A). The antiproliferative property (IC<sub>50</sub>) of **4** for non-malignant cells HK2 (18.4 ± 1.3 μM), NP69 (12.6 ± 1.6 μM), HFK Clone 22 (>25 μM) and HFK Clone 398 (>25 μM) are significantly lower than most of the above cancer cell lines (IC<sub>50</sub> < 1 μM)(Fig. 16 B).

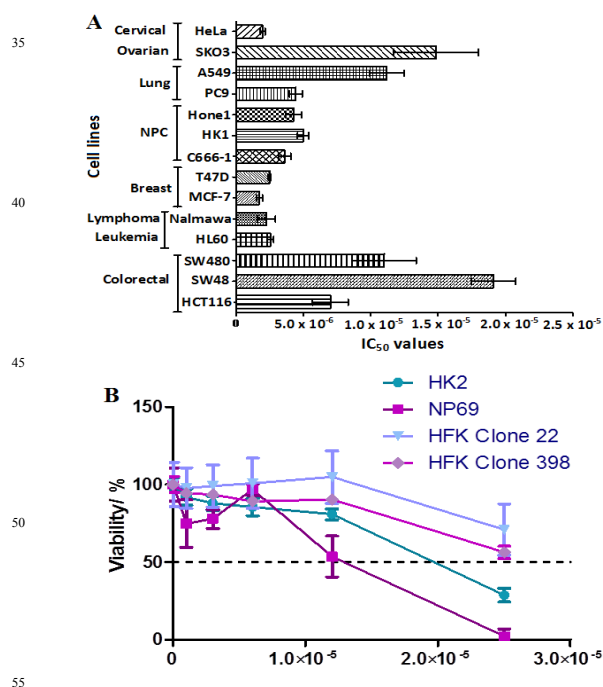


**Fig. 16** IC<sub>50</sub> values of copper(II) complex **4** for cervical (Hela), ovarian (SKOV3), lung (A549, PC9), NPC (Hone1, HK1, C666-1), breast (MCF7, T47D), lymphoma leukemia (Nalmawa, HL60) and colorectal (SW480, SW48, HCT118) cancer cell lines (A) and non-malignant cancer cell lines (B) for 24 h incubation.

Complex **4** was also send for screening on the NCI60 panel of cancer cell lines, and was accepted for a one-dose screening using sulforhodamine B assay (Sup Fig. 3).<sup>59</sup> The number reported for the one-dose assay is growth relative to no-drug control, and relative to the time zero number of cells. This allows detection of both growth inhibition (values between 0 and 100) and lethality (values less than 0). Incubation of cancer cells for 24 h with 10 μM of **4** induced more than 40% lethality (i.e. more than 40% of original cell population died) in a very high percentage cell lines in the NCI60 panel, viz. non-small cell lung cancer cells (A549/ATCC, HOP-62, HOP-92, NCI-H226, NCI-H322M, NCI-H460, NCI-H522), colon cancer cells (COLO 205, HCC-2998, HCT-15, HT29, KM12, SW-620), central nervous system cancer cells (SF-268, SF-295, SF-539, SNB-19, SNB-75, U251), melanoma cells (LOX IMVI, MALME-3M, M14, MDA-MB-435, SK-MEL-28, SK-MEL-5, UACC-257), ovarian cancer cells (OVCAR-3, OVCAR-4, OVCAR-5, OVCAR-8, SK-OV-30), renal cancer cells (789-0, A498, CAKI-1, RXT 393, SN 12C, TK-10), prostate cancer cells (DU-145), and breast cancer cells (MCF7, MDA-MB-231/ATC, BT-549, MDA-MB-468) (Sup Fig. 3). The other cell lines are more resistant and experienced lower % lethality of between 2 - 33%, and these are leukemia cells (HL-60(TB), K-562, MOLT-4, RPMI-8226, SR), colon cancer cells (HCT-116), ovarian cancer cells (IGROV1, NCI/ADR-RES), renal cancer cells (ACHN, UO-31), and breast cancer cells (HS 578T, T-47D). Overall, complex **4** is very cytotoxic to all the NCI60 cell lines, with the leukemia subpanel cell lines been more resistant. In contrast, similar one dose data of cisplatin showed no lethality and very poor or no growth inhibition of the NCI60 panel cell lines (NSC119875; Sup Fig. 4). Here, cisplatin did not induce growth inhibition in 30 cell lines while it only induced 20-40 % growth inhibition in HOP-92 (non-small cell lung) and IGROV1 (ovarian) cell lines, and less than 20% growth inhibition in the rest of the NCI60 cell lines. Hence, anticancer potency of **4** is greater than that of cisplatin for a wide range of cancers.

### Conclusions

The antiproliferative and apoptosis-inducing properties of all the [Cu(phen)(aa)(H<sub>2</sub>O)]NO<sub>3</sub> complexes **1-4** are selective towards MDA-MB-231 breast cancer cells over MCF10A non-malignant breast cells. Two of these complexes with methylated glycine (at α-carbon), viz. **2** and **4**, appear to also selectively induce cell cycle arrest at G<sub>0</sub>/G<sub>1</sub>. This selectivity may be attributed to (i) generating higher induced ROS levels in cancer cells over normal cells, and (ii) selective induction of nuclear DSBs which may result from sufficiently high ROS elevation in cancer cells. The complexes **1 - 4** were found to induce proteasome inhibition in MDA-MB-231 cells. As all the proteolytic sites of the cancer cells were not inhibited by **4**, the mechanism of proteasome inhibition is still uncertain.

The anticancer selectivity of **4** has also been established for numerous cancer cell lines over some normal cell lines. Comparison of one-dose NCI60 screening data of **4** at 10  $\mu$ M and a previously done NCI60 screening data of cisplatin revealed that **4** is much more effective than cisplatin. It was highly effective in killing almost all types of cancer cells in the NCI panel, and the potential development of **4** and the other copper(II) complexes (**1** – **3**) into useful drugs against a wide range of cancer types is suggested. By comparing the results of  $[\text{Cu}(\text{8OHQ})_2]$ , **1** – **4** and other copper(II) complexes, it seems that the combination of copper(II) and the right choice of ligand(s) may be important in discovering leads in the development of copper(II) complexes into successful anticancer drugs. Investigation into the underlying causes of why some copper(II) complexes are selective and why others are not may reveal principles needed to rationally design metal-based anticancer drugs with greater efficacy and reduced harmful side effects.

### Disclosure

C. H. Ng, S. M. Kong, S. B. Alan Khoo and A. Munirah are named patent inventors in a patent application with the Intellectual Property Corporation of Malaysia (MyIPO) which was filed on 28 June 2013 and allocated PCT Application No.PCT/MY2013/000120.

### Acknowledgements

This work is supported by MOSTI eScience grants (02-02-SF0033; 02-02-09-SF0036) and funding from Ministry of Health. We also thank the Director General of Health Malaysia for his permission to publish this article and the Director of the Institute for Medical Research (IMR) for her support. KSM expressed her appreciation to IMR, UTAR and MOSTI for use of facilities, funding and assistance in completing her MSc work. NCH would like to thank the NCI Developmental Therapeutics Program, funded by National Cancer Institute, National Institutes of Health (NIH-NCI), for the one dose 60-cell line screening of compound **4**.

### References

- 1 E. J. Gao, K. H. Wang, M. C. Zhu, L. Liu, Hairpin-shaped tetranuclear palladium(III) complex: synthesis, crystal structure, DNA binding and cytotoxicity activity studies, *Eur. J. Med. Chem.*, 2000, **45**, 2784.
- 2 D. Chen, V. Milacic, M. Frezza, Q. P. Dou, Metal complexes, their cellular targets and potential for cancer therapy, *Curr. Pharm. Des.*, 2009, **15**, 777.
- 3 U. Jungwirth, C. R. Kowol, B. K. Keppler, C. G. Hartinger, W. Berger, P. Heffeter, Anticancer activity of metal complexes: involvement of redox processes, *Antioxid. Redox. Signaling*, 2011, **15**, 1085.
- 4 A. Gupte, R. J. Mumper, Elevated copper and oxidative stress in cancer cells as a target for cancer treatment, *Cancer Treat. Rev.*, 2009, **35**, 32.

- 5 X. J. Wu, X. Hua, Targeting ROS: selective killing of cancer cells by a cruciferous vegetable derived pro-oxidant compound, *Cancer Biol. Ther.*, 2007, **6**, 646.
- 6 A. Rivero-Müller, A. D. Vizcaya-Ruiz, N. Plant, L. Ruiz, M. Dobrota, Mixed chelate copper complex, Casiopeina Ilgly<sup>R</sup>, binds and degrades nucleic acids: a mechanism of cytotoxicity, *Chem. Biol. Interact.*, 2007, **165**, 189.
- 7 G. Filomeni, G. Cerchiaro, A. M. Da Costa Ferreira, A. De Martino, J. Z. Pedersen, G. Rotilio, M. R. Ciriolo, Pro-apoptotic activity of novel isatin-Schiff base copper(II) complexes depends on oxidative stress induction and organelle-selective damage, *J. Biol. Chem.*, 2007, **16**, 12010.
- 8 A. Ganguly, S. Basu, K. Banerjee, P. Chakraborty, A. Sarkar, M. Chatterjee, S. K. Chaudhuri, Redox active copper chelate overcomes multidrug resistance in T-lymphoblastic leukemia cell by triggering apoptosis, *Mol. Biosyst.*, 2011, **7**, 1701.
- 9 J. Adams, The proteasome: a suitable antineoplastic target, *Nature Rev. Cancer*, 2004, **4**, 349.
- 10 F. Tisato, C. Marzano, M. Porchia, M. Pellei, C. Santini, Copper in diseases and treatments, and copper-based anticancer strategies, *Med. Res. Rev.*, 2010, **30**, 708.
- 11 Y. Pevzner, R. Metcalf, M. Kantor, D. Sagaro, K. Daniel, Recent advances in proteasome inhibitor discover., *Expert Opin. Drug Disc.*, 2013, **8**, 537.
- 12 M. A. Tanguy-Schmidt, M. Avenel-Audran, A. Croué, S. Lissandre, M. Dib, M. Zidane-Marinelles, M. P. Moles, Hunault-Berger, Dermatose neutrophilique aigue induite par le bortezomib, *Annales de Dermatologie et de Venerologie*, 2009, **136**, 443.
- 13 A. Kazi, H. Lawrence, W. C. Guida, M. L. McLaughlin, G. M. Springelt, N. Berndt, R. M. L. Yip, S. M. Sebti, Discovery of a novel proteasome inhibitor selective for cancer cells over non-transformed cells, *Cell Cycle*, 2009, **8**, 1940.
- 14 K.G. Daniel, P. Gupta, R.H. Harbach, W.C. Guida, Q. Ping Dou, Organic copper complexes as a new class of proteasome inhibitors and apoptosis inducers in human cancer cells, *Biochem. Pharm.*, 2004, **67**, 1139.
- 15 Z. Yu, F. Wang, V. Milacic, X. Li, Q. Cindy Cui, B. Zhang, B. Yan, Q. Ping Dou, Evaluation of copper-dependent proteasome-inhibitory and apoptosis-inducing activities of novel pyrrolidine dithiocarbamate analogues, *Int. J. Mol. Med.*, 2007, **20**, 919.
- 16 X. Zhang, C. Bi, Y. Fan, Q. Cui, D. Chen, Y. Xiao, Q. Ping Dou, Induction of tumor cell apoptosis by taurine Schiff base copper complex is associated with the inhibition of proteasomal activity, *Int. J. Mol. Med.*, 2008, **22**, 677.
- 17 S. S. Hindo, M. Frezza, D. Tomco, M. J. Heeg, L. Hryhorczuk, B. R. McGarvey, Q. Ping Dou, C. N. Verani, Metals in anticancer therapy: Copper(II) complexes as inhibitors of the 20S proteasome, *Eur. J. Med. Chem.*, 2009, **44**, 4353.
- 18 S. Zhang, J. Zhou, Ternary copper(II) complex of 1,10-phenanthroline and glycine: crystal structure and interaction with DNA, *J. Coord. Chem.*, 2008, **61**, 2488.
- 19 H. L. Seng, W. S. Wang, S. M. Kong, H. K. Alan Ong, W. F. Win, R. N. Z. Raja Abd Rahman, M. Chikira, W. K. Leong, M. Ahmad, S. B. Alan Khoo, C. H. Ng, Biological and cytoselective anticancer properties of copper(II)-polypyridyl complexes modulated by auxiliary methylated glycine ligand, *Biomaterials*, 2012, **125**, 1061.

- 1  
2  
3  
4  
5  
6  
7  
8  
9  
10  
11  
12  
13  
14  
15  
16  
17  
18  
19  
20  
21  
22  
23  
24  
25  
26  
27  
28  
29  
30  
31  
32  
33  
34  
35  
36  
37  
38  
39  
40  
41  
42  
43  
44  
45  
46  
47  
48  
49  
50  
51  
52  
53  
54  
55  
56  
57  
58  
59  
60
- 20 M. Center, A. Jemal, R. L. Siegel, Global cancer facts and figures, American Cancer Society, Atlanta, 2011, pp 1-60.
- 21 P. Fedele, A. Marino, L. Orlando, P. Schiavone, A. Nacci, F. Sponziello, P. Rizzo, N. Calvani, E. Massoni, M. Cinefra, S. Cimieri, Efficacy and low-dose metronomic chemotherapy with capicitabine in heavily treated patients with metastatic breast cancer, *Eur. J. Cancer*, 2012, **48**, 24.
- 22 N. S. El Saghir, A. Tfayli, H. A. Hatoum, Z. Nachef, P. Dinh, A. Awada, Treatment of metastatic breast cancer: state-of-art, subtypes, and perspectives, *Crit. Rev. Oncol. Hemat.*, 2011, **80**, 433.
- 23 R. M. Neve, K. Chin, J. Fridlyand, J. Yeh, F. L. Baehner, T. Fevr, L. Clark, N. Bayani, J. P. Coppe, F. Tong, T. Speed, P. T. Spellman, S. DeVries, A. Lapuk, N. J. Wang, W. L. Kuo, J. L. Stilwell, D. Pinkel, D. G. Albertson, F. M. Waldman, F. McCormick, R. B. Dickson, M. D. Johnson, M. Lippman, S. Ethier, A. Gazdar, J. W. Gray, A collection of breast cancer cell lines for the study of functionally distinct cancer subtypes, *Cancer Cell*, 2006, **10**, 515.
- 24 P. V. Shekhar, M. L. Chen, J. Werdell, G. H. Heppner, F. R. Miller, J. K. Christman, Transcriptional activation of functional endogenous estrogen receptor gene expression in MCF10A cells: a model for early breast cancer, *Int. J. Oncol.*, 1998, **13**, 907.
- 25 F. R. Miller, H. D. Soule, L. Tait, R. J. Pauley, S. R. Wolman, P. J. Dawson, G. H. Heppner, Xenograft model of progressive human breast disease, *J. Natl. Cancer Inst.*, 1993, **85**, 1725.
- 26 S. Van Cruchten, W. Van Den Broeck, Morphological and biological aspects of apoptosis, oncosis, and necrosis, *Anat. Histol. Embryol.*, 2002, **31**, 214.
- 27 J. F. Kerr, A. H. Wyllie, A. R. Currie, Apoptosis: a basic biological phenomenon with wide ranging implications in tissue kinetics, *Br. J. Cancer*, 1972, **26**, 239.
- 28 F. B. Do Nascimento, G. Von Peelsitz, F. R. Pavan, D. N. Sato, C. W. F. Leite, H.S. Selistre-de-Araújo, J. Ellena, E. E. Castellano, V. M. Deflon, A. A. Batista, Synthesis, characterization, X-ray structure and *in vitro* antimycobacterial and antitumoral activities of Ru(II) phosphine/diimine complexes containing the "SpymMe<sub>2</sub>" ligand, SpymMe<sub>2</sub> = 4,6-dimethyl-2-mercaptopyrimidine, *J. Inorg. Biochem.*, 2008, **102**, 1783.
- 29 S. Rubino, P. Portanova, A. Girasolo, G. Calvaruso, S. Orecchio, G. C. Stocco, Synthetic, structural and biochemical studies of polynuclear platinum(II) complexes with heterocyclic ligands, *Eur. J. Med. Chem.*, 2009, **44**, 1041.
- 30 R. Schobert, S. Seibt, K. Mahal, A. Ahmad, B. Biersack, K. Effenberger-Neidnicht, S. Padhye, F. H. Sarkar, T. Mueller, Cancer selective metallocenedicarboxylates of the fungal cytotoxin Illudin M, *J Med Chem.*, 2011, **54**, 6177.
- 31 R. Cathcart, E. Schwiers, B. N. Ames, Detection of picomole of hydroperoxides using a fluorescent dichlorofluorescein assay, *Anal Biochem.*, 1983, **134**, 111.
- 32 C. V. Pereira, S. Nadanaciva, P. J. Oliveira, Y. Will, *Exp Opin. Drug Metab. Toxicol.*, 2012, **8**, 219.
- 33 J. Zheng, J. R. Lou, X. X. Zhang, D. M. Benbrook, M. H. Hanigan, S. E. Lind, W. Q. Ding, N-Acetylcysteine interacts with copper to generate hydrogen peroxide and selectively induce cancer cell death, *Cancer Lett.*, 2010, **298**, 186.
- 34 N. Y. Min, J. H. Kim, J. H. Choi, W. Liang, Y. J. Ko, S. Rhee, H. Bang, S. W. Ham, A. J. Park, K. H. Lee, Selective death of cancer cells by preferential induction of reactive oxygen species in response to (-)-epigallocatechin-3-gallate, *Biochem. Biophys. Res. Commun.*, 2012, **421**, 91.
- 35 C. Deegan, B. Coyle, M. McCann, M. Devereux, D. A. Egan, *In vitro* anti-tumour effect of 1,10-phenanthroline-5,6-dione (phenidione), [Cu(phenidione)<sub>3</sub>](ClO<sub>4</sub>)<sub>2</sub>·4H<sub>2</sub>O and [Ag(phenidione)<sub>2</sub>]ClO<sub>4</sub> using human epithelial cell lines, *Chem-Biol. Interact.*, 2006, **164**, 115.
- 36 P. T. Schumacker, Reactive oxygen species in cancer cells: live by the sword, die by the sword, *Cancer Cell*, 2006, **10**, 175.
- 37 P. Heffeter, M. A. Jakupec, W. Kömer, S. Wild, N. G. von Keyserlingk, L. Elbling, H. Zorbass, A. Korynevskaya, S. Knasmüller, H. Sutterlüty, M. Micksche, B. K. Keppler, W. Berger, Anticancer activity of the lanthanum compound [tris(1,10-phenanthroline)lanthanum(III)] trithiocyanate, *Biochem. Pharmacol.*, 2006, **71**, 426.
- 38 R. I. Yarden, S. Metsuyanım, I. Pickholtz, S. Shabbeer, H. Tellio, M. Z. Papa, BRCA1-dependent Chk1 phosphorylation triggers partial chromatin dissociation of phosphorylated Chk1 and facilitates S-phase cell cycle arrest, *Int. J. Biochem. Cell Biol.*, 2012, **44**, 1761.
- 39 U. Olszewski, F. Ach, E. Ulsperger, G. Baumgartner, R. Zeillinger, P. Bednarski, G. Hamilton, In vitro evaluation of oxaplatin: an oral platinum(IV) anticancer drug, *Metal-Based Drugs*, 2009, **2009**, 1.
- 40 J. Serment-Guerrero, P. Cano-Sanchez, E. Reyes-Perez, F. Velazquez-Garcia, M. E. Bravo-Gomez, L. Ruiz-Azuara, Genotoxicity of the copper antineoplastic coordination complexes casiopienas<sup>®</sup>, *Toxicol. Vitro.*, 2011, **25**, 1376.
- 41 C. H. Ng, H. K. Alan Ong, C. W. Kong, K. W. Tan, R. N. Z. Raja Abd. Rahman, B. M. Yamin, S. W. Ng, Factors affecting the nucleolytic cleavage of DNA by (N,N-ethylenediaminediacetato)-metal(II) complexes, M(edda). Crystal structure of Co(edda), Polyhedron, 2006, **25**, 3118.
- 42 H. L. Seng, H. K. Alan Ong, R. N. Z. Raja Abd. Rahman, B. M. Yamin, E. R. T. Tiekink, K. W. Tan, M. J. Maah, L. Caracelli, C. H. Ng, *J. Inorg. Biochem.*, 2008, **102**, 1997.
- 43 J. Annaraj, S. Srinivasan, K. M. Ponvel, P. R. Athappan, Mixed ligand copper(II) complexes of phenanthroline/bipyridyl and curcumin diketimines as DNA intercalators and their electrochemical behavior under Nafion<sup>®</sup> and clay modified electrodes, *J. Inorg. Biochem.*, 2005, **99**, 669.
- 44 C. Liu, J. Zhou, Q. Li, L. Wang, Z. Liao, H. Xu, DNA damage by copper(II) complexes: coordination-structural dependent reactivities, *J. Inorg. Biochem.*, 1999, **75**, 233.
- 45 Y. Wang, X. Zhang, Q. Zhang, Z. Yang, Oxidative damage to by 1,10-phenanthroline/L-threonine copper(II) complexes with chlorogenic acid, *Biomaterials*, 2010, **23**, 265.
- 46 N. Srivastava, S. Gochhait, P. de Boer, R. N. Bamezai, Role of H2AX in DNA damage response and human cancers, *Mutat. Res.*, 2009, **68**, 180.
- 47 B. Mukherjee, C. Kessinger, J. Kobayashi, B. P. Chen, D. J. Chen, A. Chatterjee, S. Burma, DNA-PK phosphorylates histone H2AX during apoptotic DNA fragmentation in mammalian cells, *DNA Repair*, 2006, **5**, 575.
- 48 X. Huang, Z. Darzynkiewicz, Cytometric assessment of H2AX phosphorylation, *Mds. Mol. Biol.*, 2006, **314**, 73.
- 49 T. Tanaka, X. Huang, H. D. Halicka, H. Zhao, F. Traganos, A. P. Albino, W. Dai, Z. Darzynkiewicz, Cytometry of ATM activation

- and histone H2AX phosphorylation to estimate extent of DNA damage induced by exogenous agents, *Cytometry A.*, 2007, **71**, 648.
- 50 M. L. Circu, T. W. Aw, Reactive oxygen species, cellular redox system and apoptosis, *Free Rad. Biol. Med.*, 2010, **48**, 749.
- 51 T. Jung, B. Catalgol, T. Grune, Proteasomal system, *Mol. Aspects Med.*, 2009, **30**, 191.
- 52 L. Meng, R. Mohan, B. H. B. Kwok, M. Elofsson, N. Sin, C. M. Crews, Epoxomicin, a potent and selective proteasome inhibitor, exhibits in vivo anti-inflammatory activity, *Proc. Natl. Acad. Sci.*, 1999, **96**, 10403.
- 53 A. Collavoli, L. Comelli, T. Cervalli, A. Galli. The Over-expression of the  $\beta 2$  catalytic subunit of the proteasome decreases homologous recombination and impairs DNA double-strand break repair in human cells, *J. Biomed. Biotech.*, 2011, Article ID 757960.
- 54 J. Zuo, C. Bi, Y. Fan, D. Buac, C. Nardon, K. G. Daniel, Q. Ping Dou, Cellular and computational studies of proteasome inhibition and apoptosis induction in human cancer cells by amino acid-Schiff base-copper complexes, *J. Inorg. Biochem.*, 2013, **118**, 83.
- 55 B. Cvek, V. Milacic, J. Taraba, Q. P. Dou, Ni(II), Cu(II), and Zn(II) diethyldithiocarbamate complexes show various activities against the proteasome in breast cancer cells, *J. Med. Chem.*, 2008, **51**, 6256.
- 56 H.S. Lim, C. T. Archer, T. Kodedek, Identification of a peptoid inhibitor of the proteasome 19S regulatory particle, *J. Am. Chem. Soc.*, 2007, **129**, 7750.
- 57 T. Hideshima, D. Chauhan, P. Richardson, C. Mitsiades, N. Mitsiades, T. Hayashi, N. Munshi, L. Dong, A. Castro, V. Palombella, J. Adams, K. C. Anderson, NF- $\kappa$ B as a Therapeutic Target in Multiple Myeloma, *J. Biol. Chem.*, 2002, **277**, 16639.
- 58 D. Hempel, M. Z. Wojtukiewicz, L. Kozlowski, J. Romatowski, H. Ostrowska, Increased plasma proteasome chymotrypsin-like activity in patients with advanced solid tumors, *Tumor Biol.*, 2011, **32**, 753.
- 59 A. Monks, D. Scudiero, P. Skehan, R. Shoemaker, K. Paull, D. Vistica, C. Hose, J. Langley, P. Cronise, A. Vaigro-Wolff, M. Gray-Goodrich, H. Campbell, J. Mayo, M. Boyd, Feasibility of a high-flux anticancer drug screen using a diverse panel of cultured human tumor cell lines, *J. Natl. Cancer Inst.*, 1991, **83**, 757.

<sup>a</sup> Department of Pharmaceutical Chemistry, School of Pharmacy, International Medical University, Bukit Jalil, 57000 Kuala Lumpur, Malaysia. Fax: 603 8656 7229; Tel: 603 2731 7483; E-mail: NgChewHee@imu.edu.my

<sup>b</sup> Faculty of Science, Universiti Tunku Abdul Rahman, 31900 Kampar, Perak, Malaysia. Fax: 605 466 1676; Tel: 605 468 8888; E-mail: siewmingkong@yahoo.com

<sup>c</sup> School of Postgraduate Studies and Research, School of Medicine, International Medical University, Bukit Jalil, 57000 Kuala Lumpur, Malaysia. Fax: 603 8656 7229; Tel: 603 2731 7483; E-mail: yeeliangtiong@gmail.com

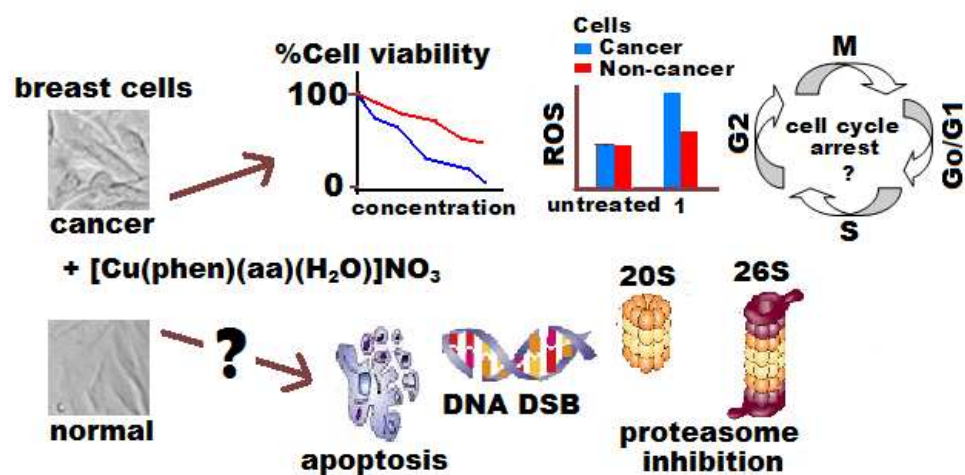
<sup>d</sup> Chemistry Department, University of Malaya, 50603 Kuala Lumpur, Malaysia. Fax: 60379674193; Tel: 60379676750. Email: jamil@mosti.gov.my

<sup>e</sup> Molecular Pathology Unit, Cancer Research Centre, Institute for Medical Research, 50588 Kuala Lumpur, Malaysia. Fax: 603 2616 2536; Tel: 603 2616 2728. Email: wanie\_gurl87@hotmail.com, alankhoo@imr.gov.my; munirah@imr.gov.my

† Electronic Supplementary Information (ESI) available: The supplementary data contain (i) Morphological observations of MDA-MB-231 and MCF10A cells which are untreated or treated with various concentrations of copper(II) compounds for 24 h (Sup Fig. 1.1-1.5 A and

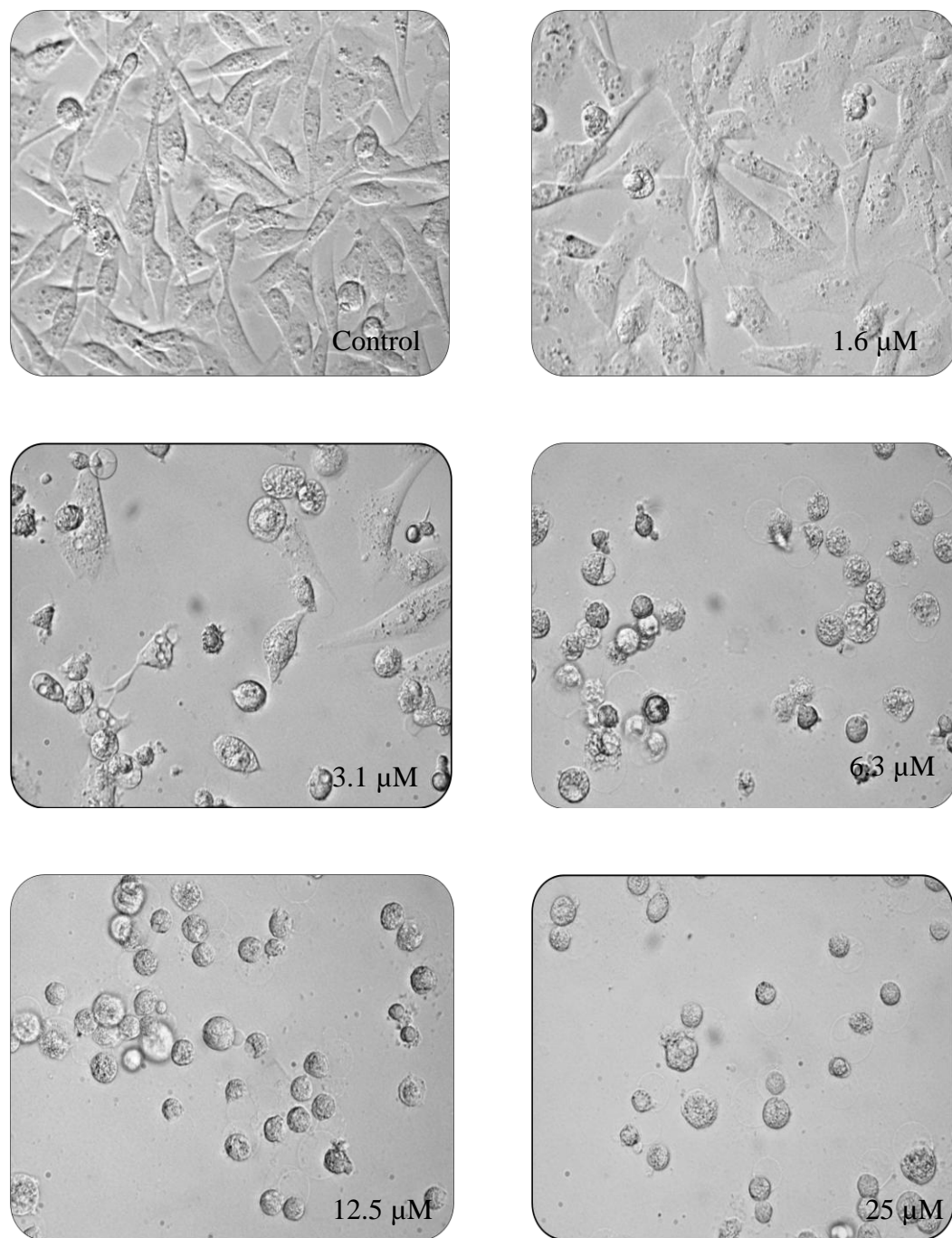
B); (ii) A comparison between untreated and treated MDA-MB-231 and MCF10A cells in expression of apoptosis after incubation with 5  $\mu$ M copper(II) complexes at 24 h by flow cytometry analysis (Sup Figs. 2.1 and 2.2); (iii) One dose NCI60 screening data of **4** and cisplatin (Sup Figs. 3 and 4 respectively); (iv) Statistical analysis of the cell cycle analysis after cells treated with copper(II) complexes **1** - **4** at 24h (Sup Table 1).

## Graphical abstract

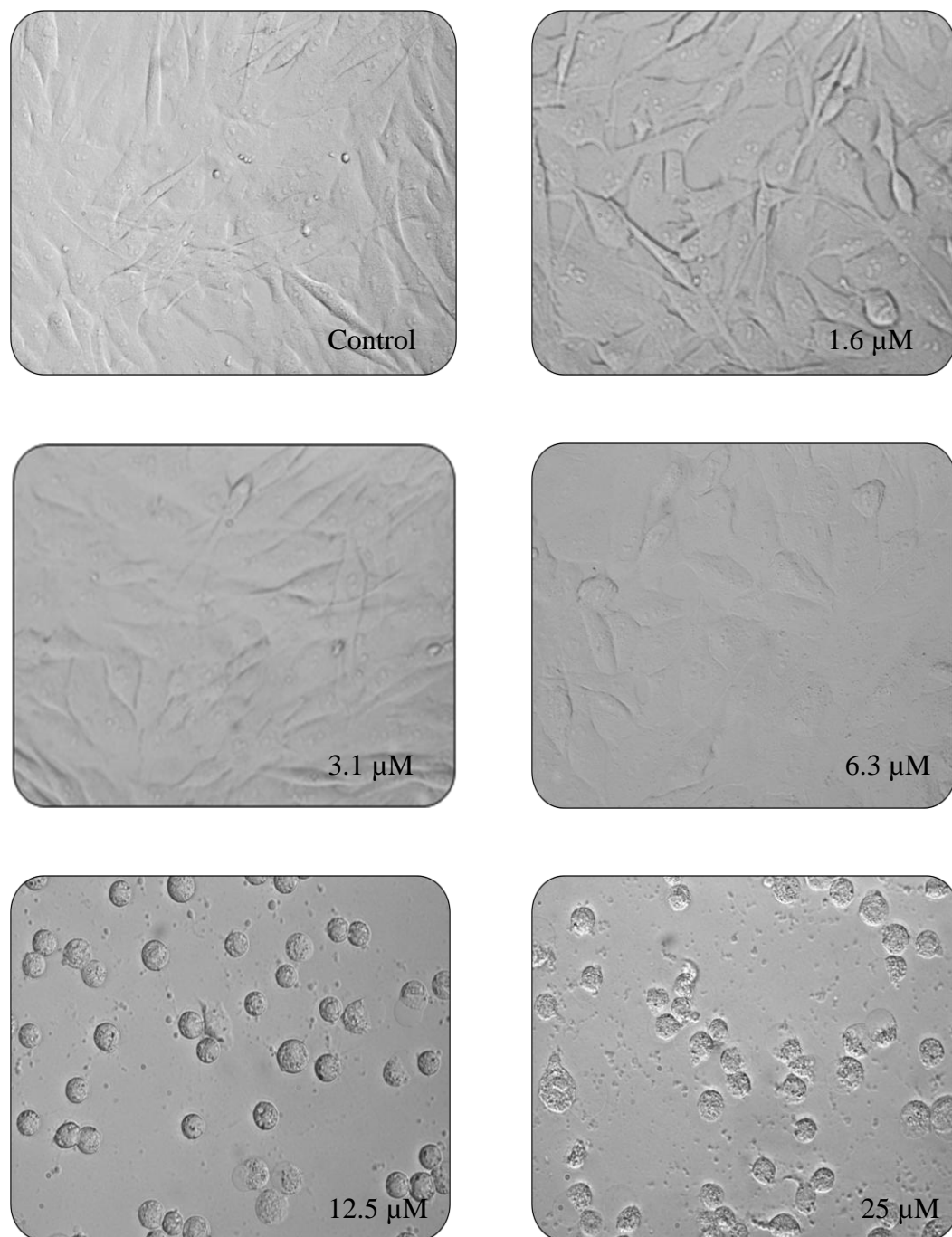


Copper(II) complexes  $[\text{Cu}(\text{phen})(\text{aa})(\text{H}_2\text{O})]\text{NO}_3 \cdot x\text{H}_2\text{O}$  **1 - 4** exhibited anticancer selectivity, as evidenced by MTT assay, % apoptosis, cell cycle arrest, ROS induction and DNA DSBs. All complexes inhibited proteasome of cancer cells but only poorly 20S chymotrypsin-like activity. NCI60 one dose screening of **4** showed it to be effective against all cell lines.

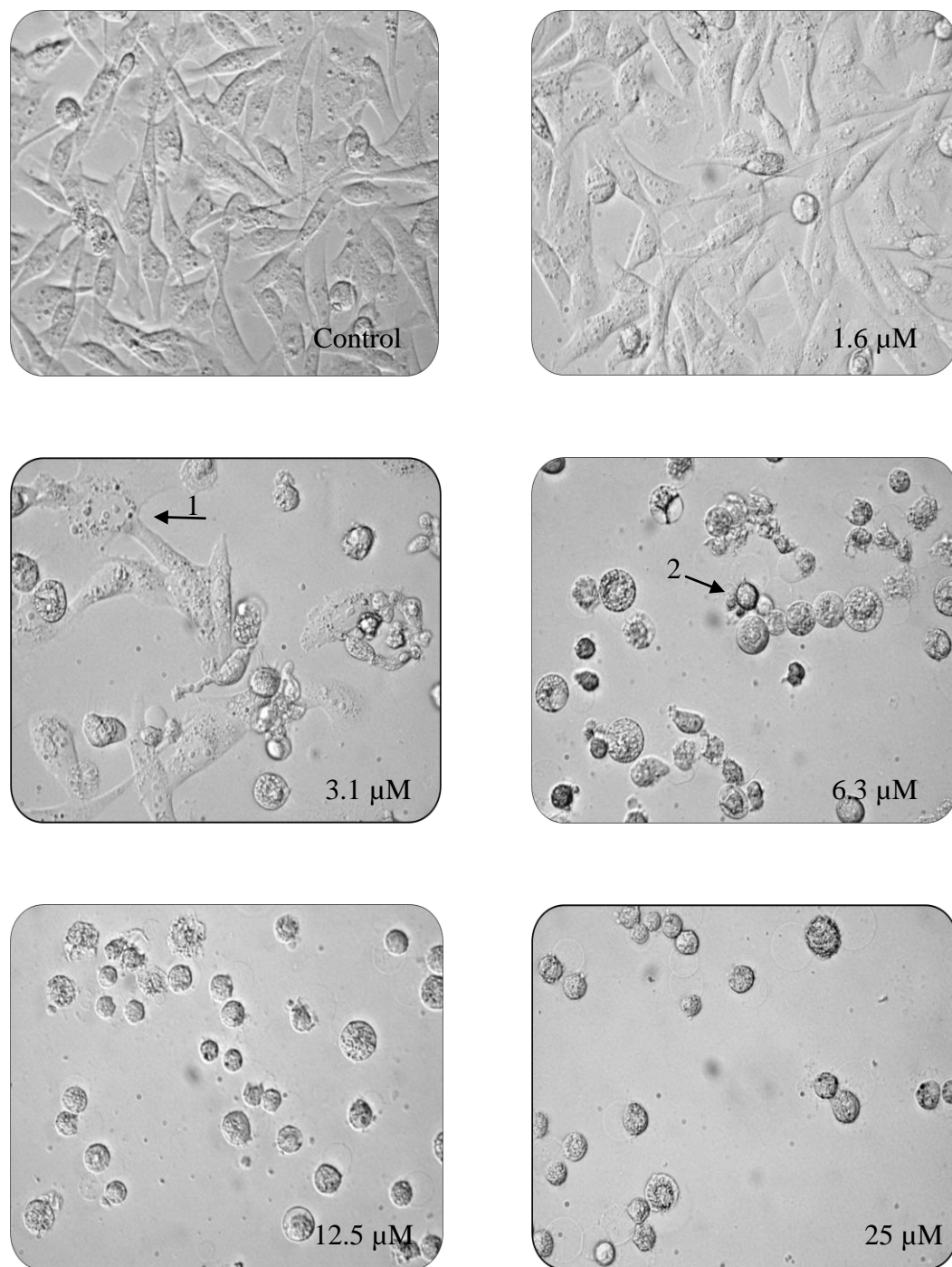
## Supplementary Figures 1.1-1.5, 2.1-2.2, 3 and 4; Supplementary Table 1



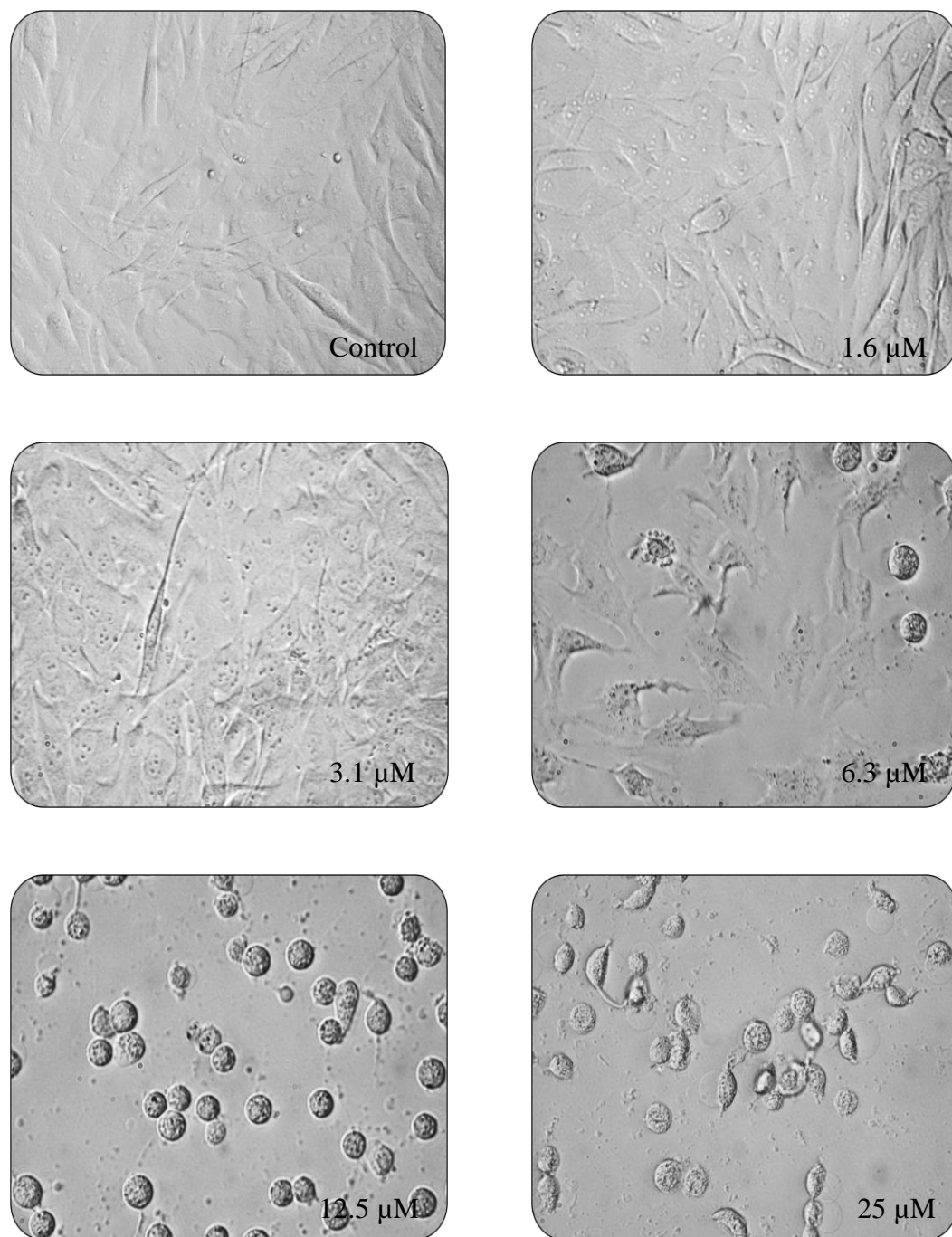
**Sup Fig. 1.1A** Morphological changes in MDA-MB-231 cells treated for 24 h with [Cu(phen)(gly)(H<sub>2</sub>O)]NO<sub>3</sub> 1 at different concentrations as compared to untreated cells. (Microscope magnification 400x). All pictures are typical of three independent experiments each performed under identical conditions.



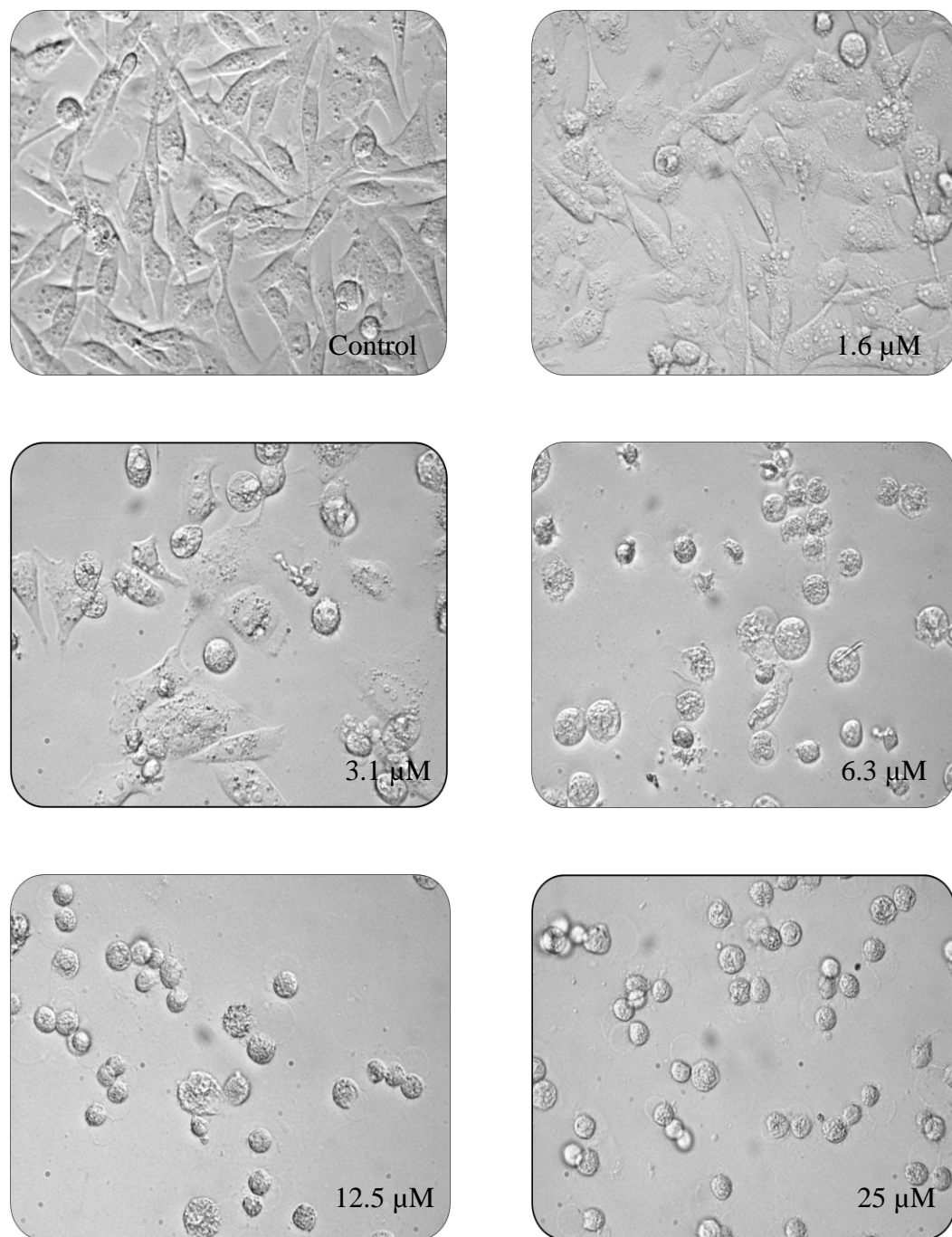
**Sup Fig. 1.1B** Morphological changes in MCF10A cells treated for 24 h with [Cu(phen)(gly)(H<sub>2</sub>O)]NO<sub>3</sub> 1 at different concentrations as compared to untreated cells. (Microscope magnification 400x). All pictures are typical of three independent experiments each performed under identical conditions.



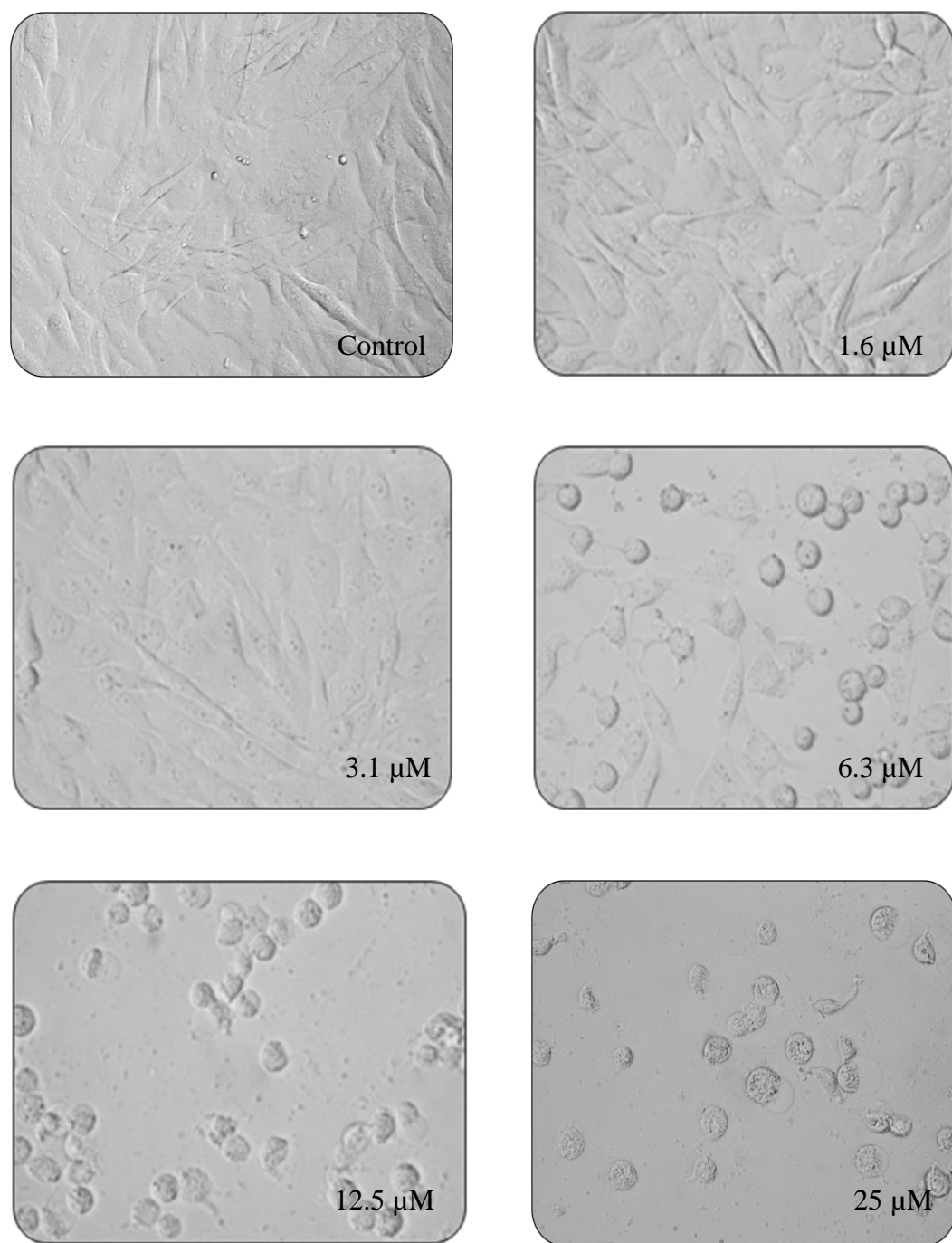
**Sup Fig. 1.2A** Morphological changes in MDA-MB-231 cells treated for 24 h with  $[\text{Cu}(\text{phen})(\text{DL-ala})(\text{H}_2\text{O})]\text{NO}_3$  **2** at different concentrations as compared to untreated cells. (Microscope magnification 400x). All pictures are typical of three independent experiments each performed under identical conditions. Arrow (1) condensation of chromatin, (2) membrane bleb.



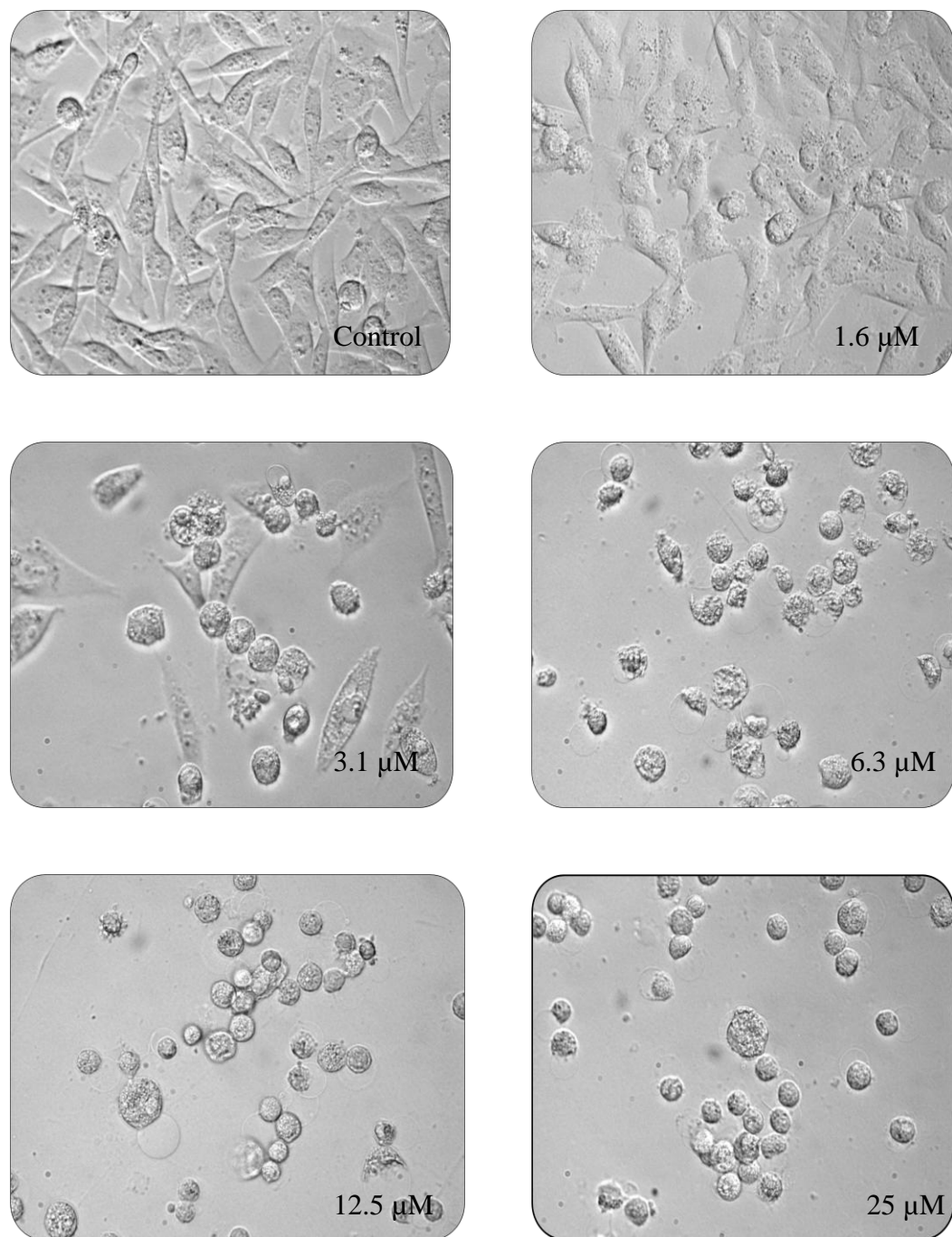
**Sup Fig. 1.2B** Morphological changes in MCF10A cells treated for 24 h with  $[\text{Cu}(\text{phen})(\text{DL-ala})(\text{H}_2\text{O})]\text{NO}_3$  **2** at different concentrations as compared to untreated cells. (Microscope magnification 400x). All pictures are typical of three independent experiments each performed under identical conditions.



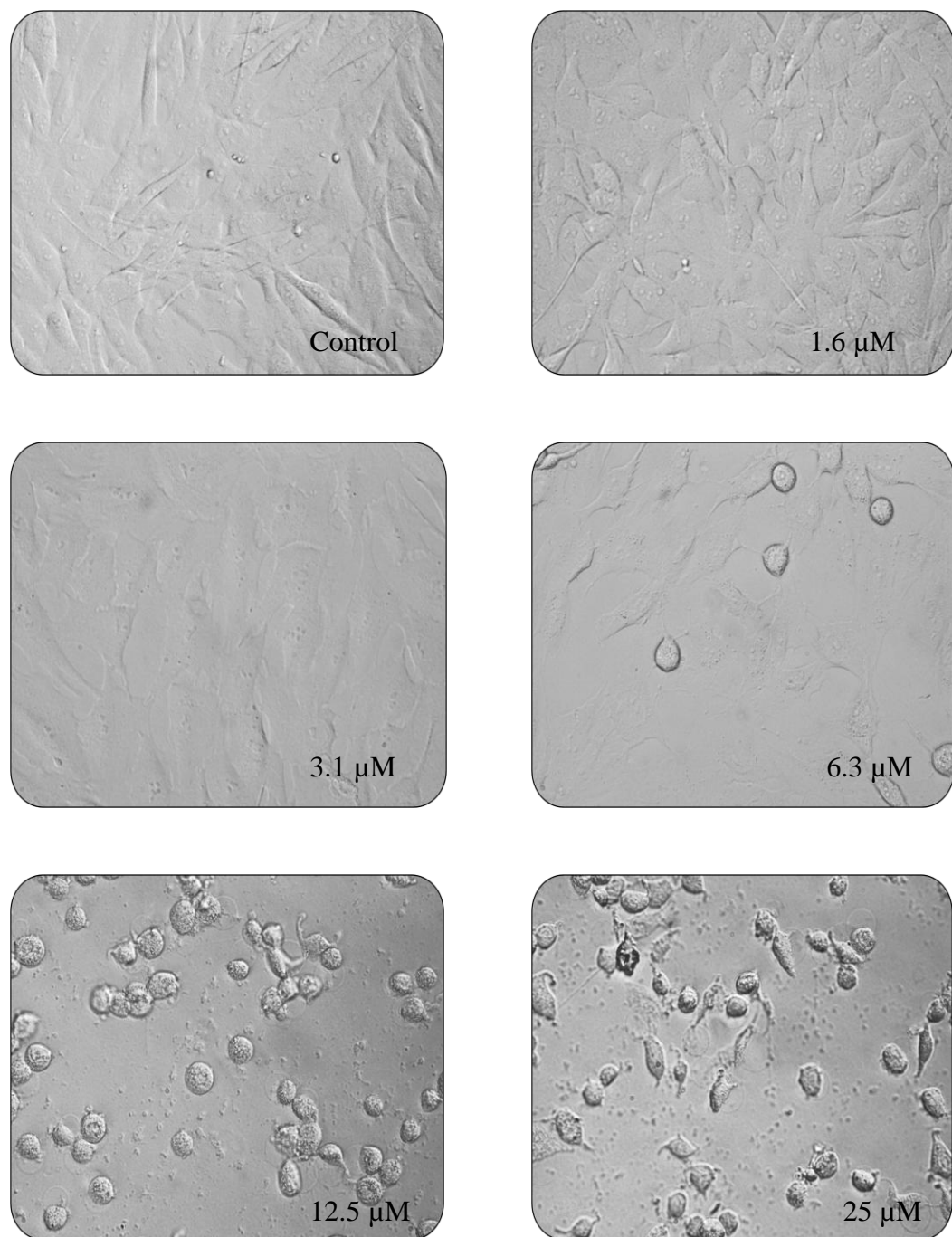
**Sup Fig. 1.3A** Morphological changes in MDA-MB-231 cells treated for 24 h with  $[\text{Cu}(\text{phen})(\text{sar})(\text{H}_2\text{O})]\text{NO}_3$  **3** at different concentrations as compared to untreated cells. (Microscope magnification 400x). All pictures are typical of three independent experiments each performed under identical conditions.



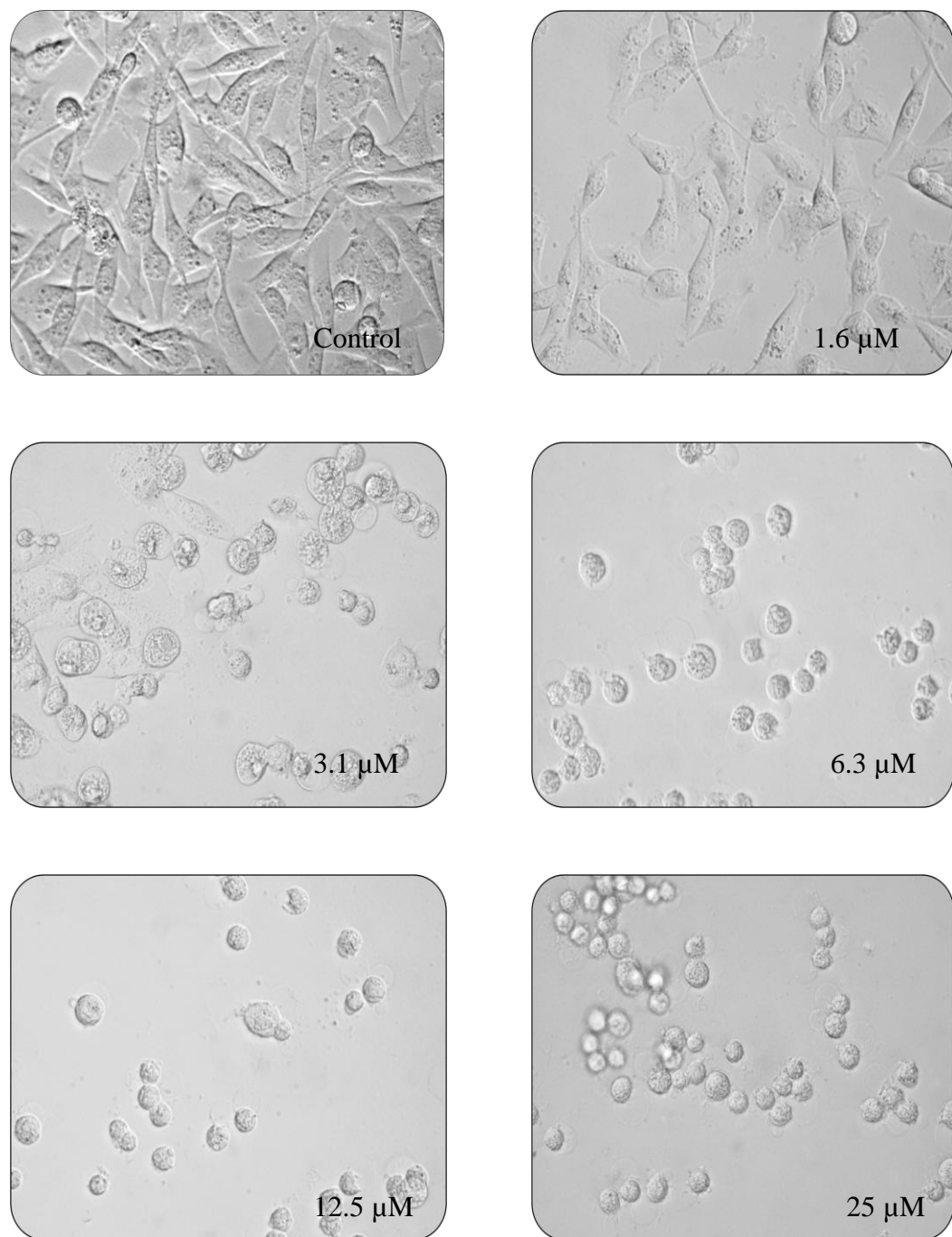
**Sup Fig. 1.3B** Morphological changes in MCF10A cells treated for 24 h with  $[\text{Cu}(\text{phen})(\text{sar})(\text{H}_2\text{O})]\text{NO}_3$  **3** at different concentrations as compared to untreated cells. (Microscope magnification 400x). All pictures are typical of three independent experiments each performed under identical conditions.



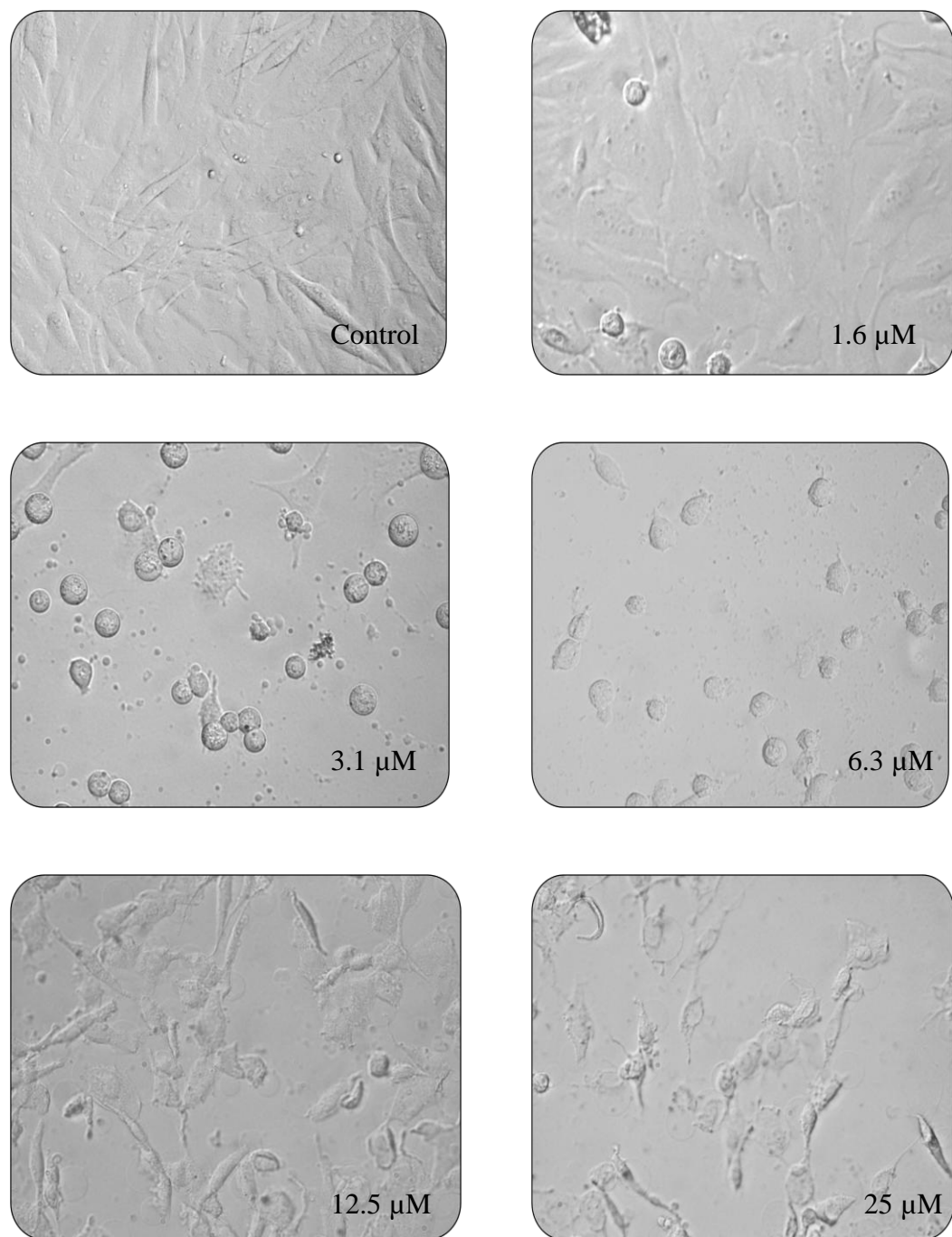
**Sup Fig. 1.4A** Morphological changes in MDA-MB-231 cells treated for 24 h with  $[\text{Cu}(\text{phen})(\text{C-dMg})(\text{H}_2\text{O})]\text{NO}_3$  **4** at different concentrations as compared to untreated cells. (Microscope magnification 400x). All pictures are typical of three independent experiments each performed under identical conditions.



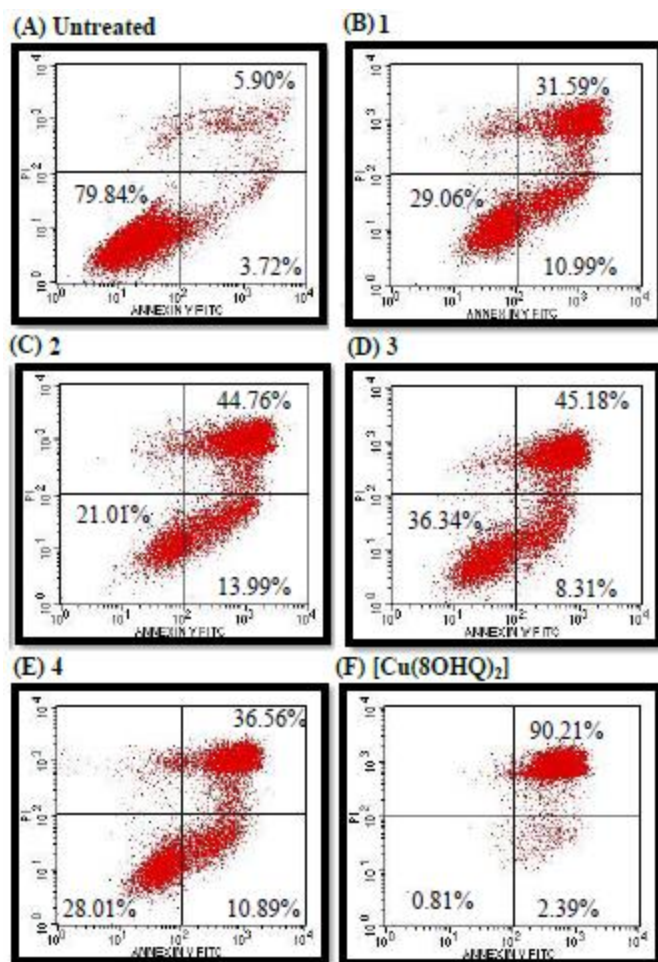
**Sup Fig. 1.4B** Morphological changes in MCF10A cells treated for 24 h with  $[\text{Cu}(\text{phen})(\text{C-dMg})(\text{H}_2\text{O})]\text{NO}_3$  **4** at different concentrations as compared to untreated cells. (Microscope magnification 400x). All pictures are typical of three independent experiments each performed under identical conditions.



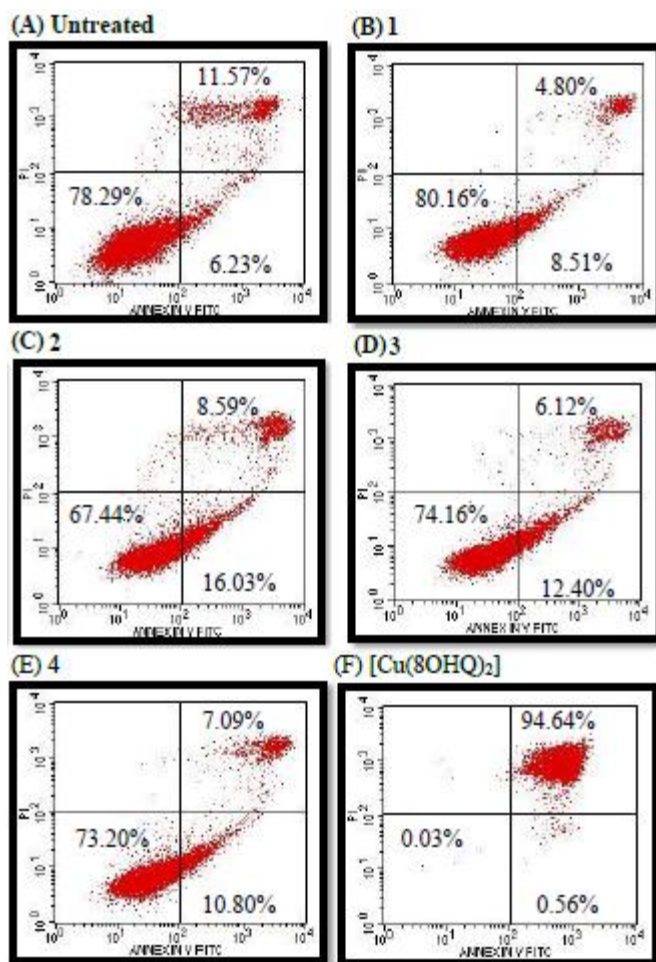
**Sup Fig. 1.5A** Morphological changes in MDA-MB-231 cells treated for 24 h with  $[\text{Cu}(\text{8OHQ})_2]$  at different concentrations as compared to untreated cells. (Microscope magnification 400x). All pictures are typical of three independent experiments each performed under identical conditions.



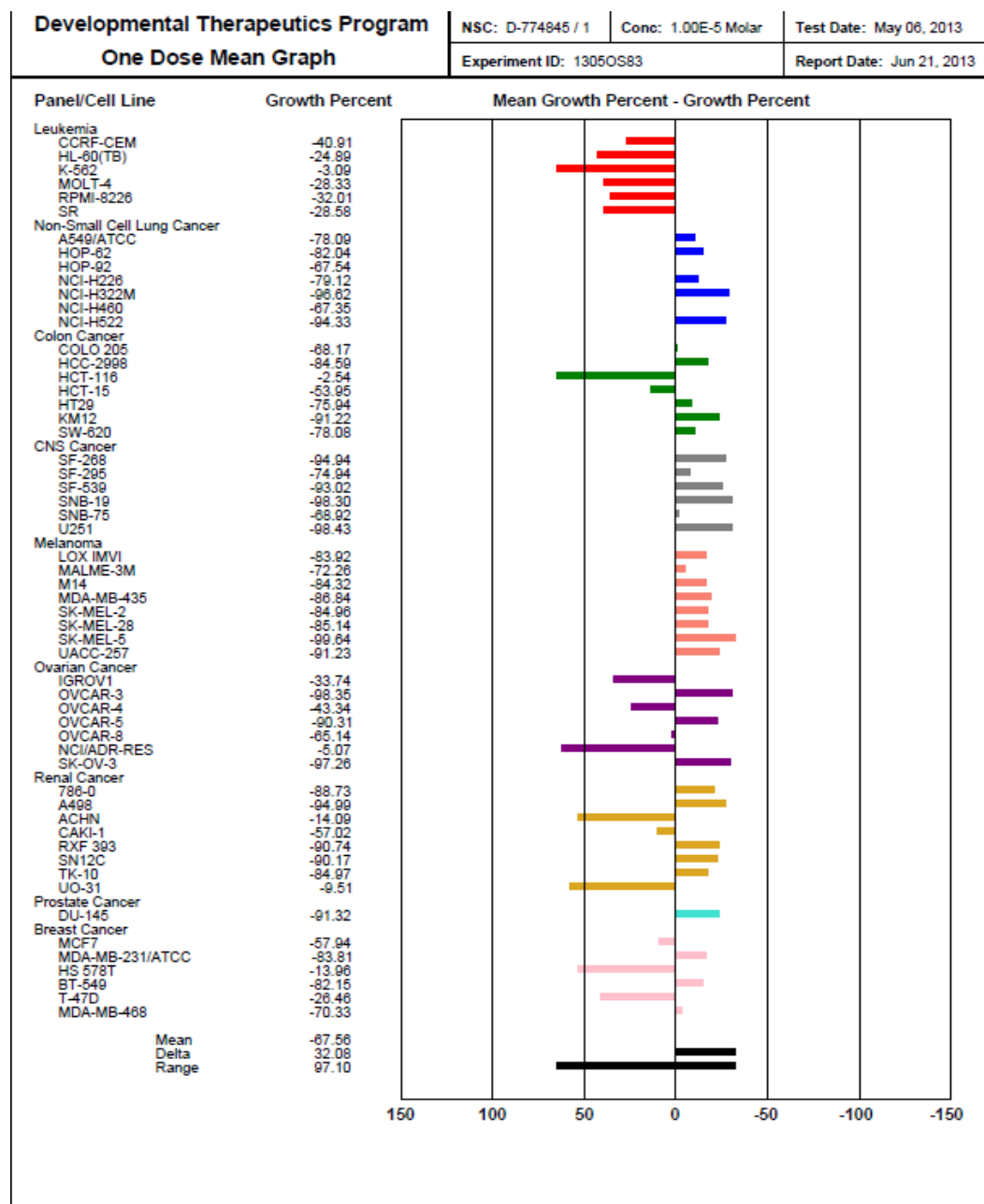
**Sup Fig. 1.5B** Morphological changes in MCF10A cells treated for 24 h with [Cu(8OHQ)<sub>2</sub>] at different concentrations as compared to untreated cells. (Microscope magnification 400x). All pictures are typical of three independent experiments each performed under identical conditions.



**Sup Fig. 2.1.** A comparison between untreated and treated MDA-MB-231 cells in expression of apoptosis after incubation with 5  $\mu$ M copper(II) complexes at 24 h by flow cytometry analysis. Percentage of total cells is shown for each quadrant. Results are representative of three independent experiments.

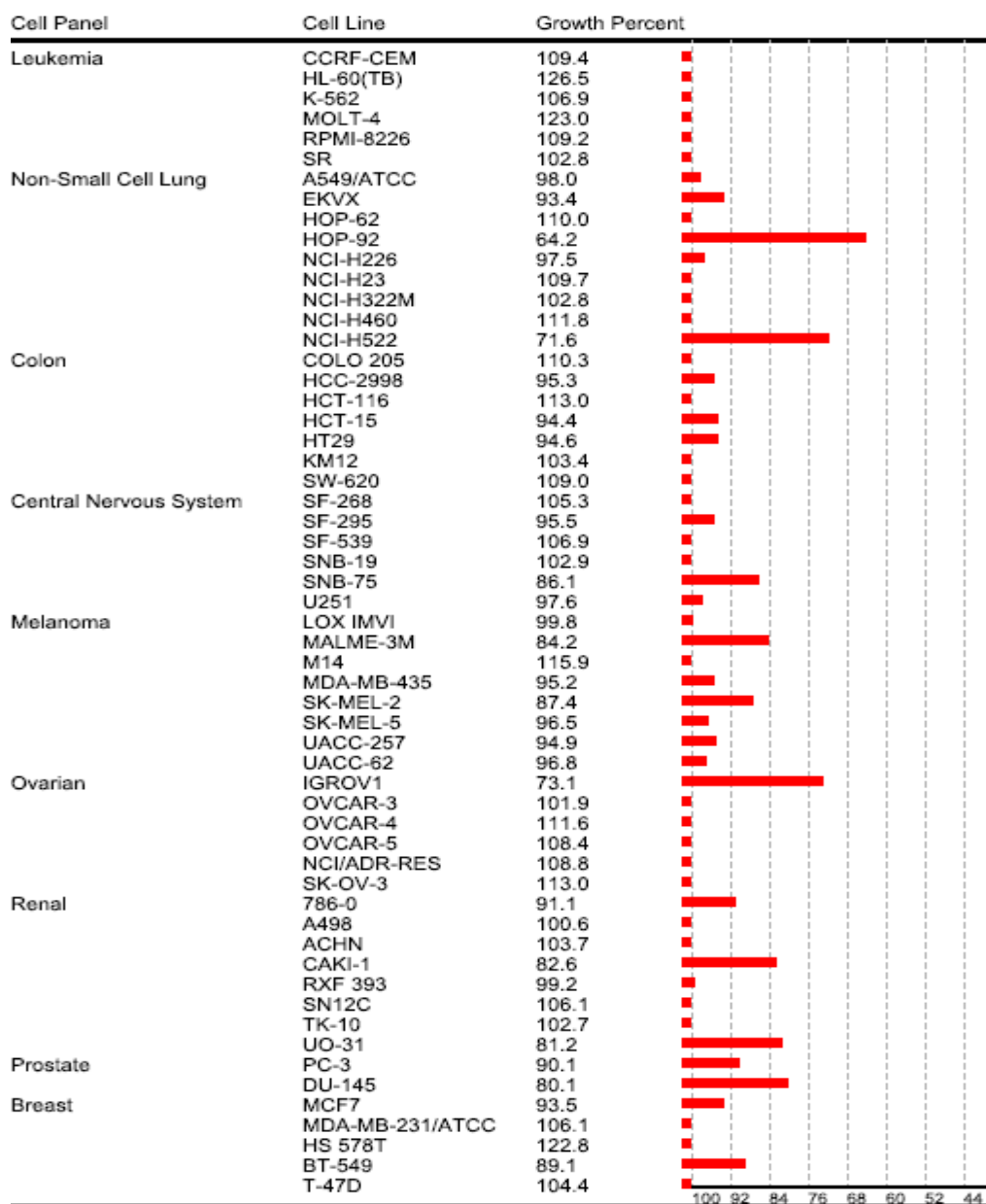


**Sup. Fig. 2.2** A comparison between untreated and treated MCF10A cells in expression of apoptosis after incubation with 5  $\mu$ M copper(II) complexes at 24 h by flow cytometry analysis. Percentage of total cells is shown for each quadrant. Results are representative of three independent experiments.



**Sup. Fig. 3** One-dose data in the National Cancer Institute anticancer screen showing a mean graph of the percent growth of cancer cells treated with of  $10 \mu\text{M}$  of **4** for 24 h. The number reported for the One-dose assay is growth relative to the no-drug control, and relative to the time zero number of cells. This allows detection of both growth inhibition (values between 0 and 100) and lethality (values less than 0). For example, a value of 100 means no growth inhibition. A value of 40 would mean 60% growth inhibition. A value of 0 means no net growth over the course of the experiment. A value of -40 would mean 40% lethality. A value of -100 means all cells are dead.

One Dose Data Graph for NSC 119875  
DTP OneDose/Syn/60 Cell Line



**Sup. Fig. 4** One-dose data in the National Cancer Institute anticancer screen showing a mean graph of the percent growth of cancer cells treated with of 10  $\mu$ M of **cisplatin** for 24 h. The number reported for the One-dose assay is growth relative to the no-drug control, and relative to the time zero number of cells. This allows detection of both growth inhibition (values between 0 and 100) and lethality (values less than 0). For example, a value of 100 means no growth inhibition. A value of 40 would mean 60% growth inhibition. A value of 0 means no net growth over the course of the experiment. A value of -40 would mean 40% lethality. A value of -100 means all cells are dead.

**Supplementary Table 1** Statistical analysis of the cell cycle analysis after cells treated with copper(II) complexes **1 - 4** at 24h. \* = (p < 0.05), \*\* = (p < 0.01), \*\*\* = (p < 0.005) indicates significantly different from untreated. NS = non-significant.

	MDA-MB-231 cells			MCF10A cells		
	G <sub>0</sub> /G <sub>1</sub> phase	S phase	G <sub>2</sub> /M phase	G <sub>0</sub> /G <sub>1</sub> phase	S phase	G <sub>2</sub> /M phase
Untreated vs <b>1</b>	NS	NS	***	NS	NS	NS
Untreated vs <b>2</b>	**	*	***	NS	**	NS
Untreated vs <b>3</b>	NS	NS	***	*	***	NS
Untreated vs <b>4</b>	*	NS	***	NS	*	NS